Update on parameterisation of major source functions, including extreme conditions.
Wave climate and wave coupled effects in atmosphere and ocean

Alex Babanin

Centre for Ocean Engineering, Science and Technology

Swinburne University, Melbourne, Australia

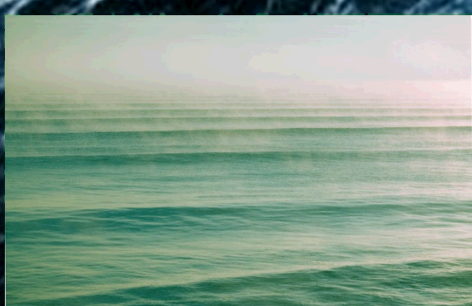

Reading, England
25 June 2012

SWINBURNE UNIVERSITY OF TECHNOLOGY

Further Motivation

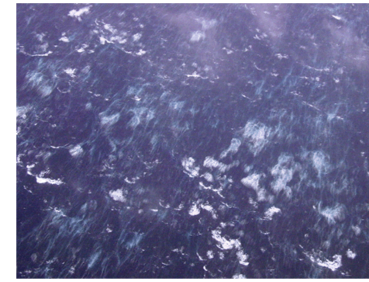

Waves and weather, extreme weather, ocean circulation, climate

Saturation of the sea drag

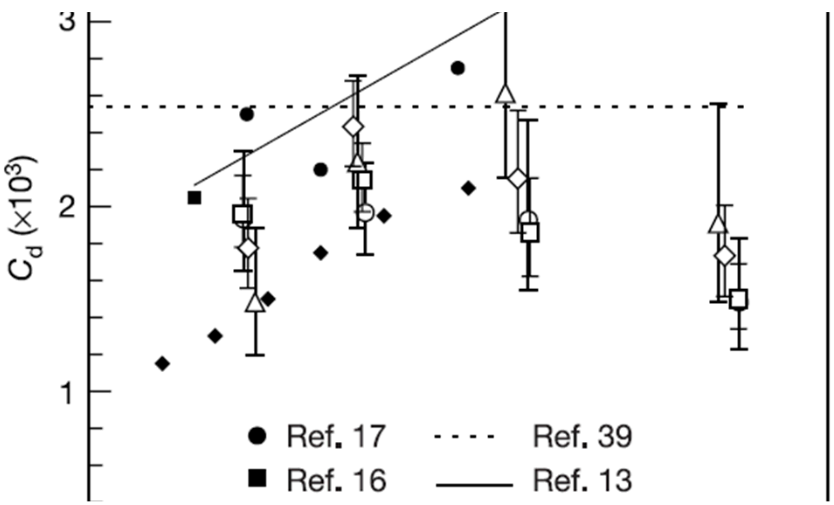

Powel et al., Nature, 2003

Sea surface temperature changes due to waves

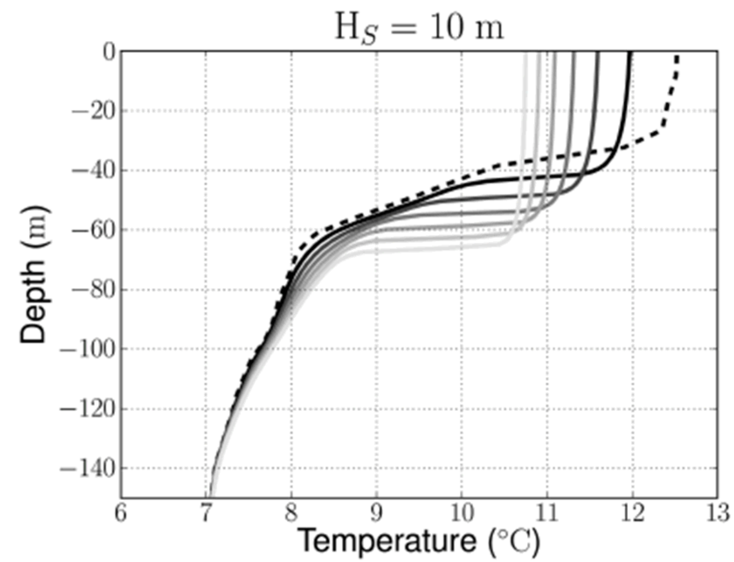

Ghantous and Babanin, Ocean Modelling, submitted

$$\frac{dE(k,f,\theta,x,t)}{dt} = S_{tot} = S_{in} + S_{ds} + S_{nl} + S_{bf}$$

Wind Input following the waves

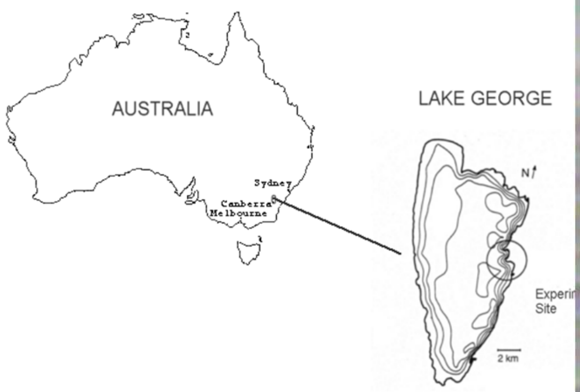

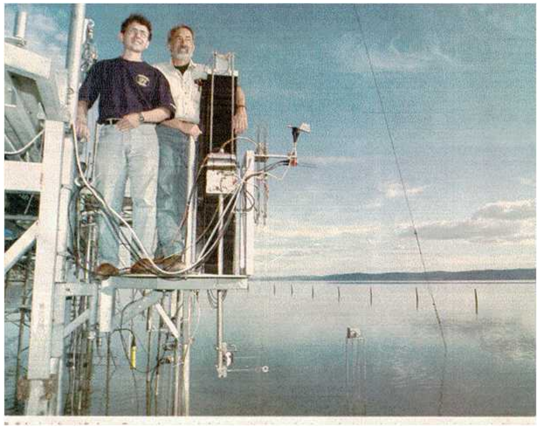

Young et al., JAOT, 2005, Donelan et al., JAOT, 2005, JPO, 2006, Babanin et al., JPO, 2007

$$\frac{dE(k,f,\theta,x,t)}{dt} = S_{in} + S_{ds} + S_{nl} + S_{bf}$$

The full separation

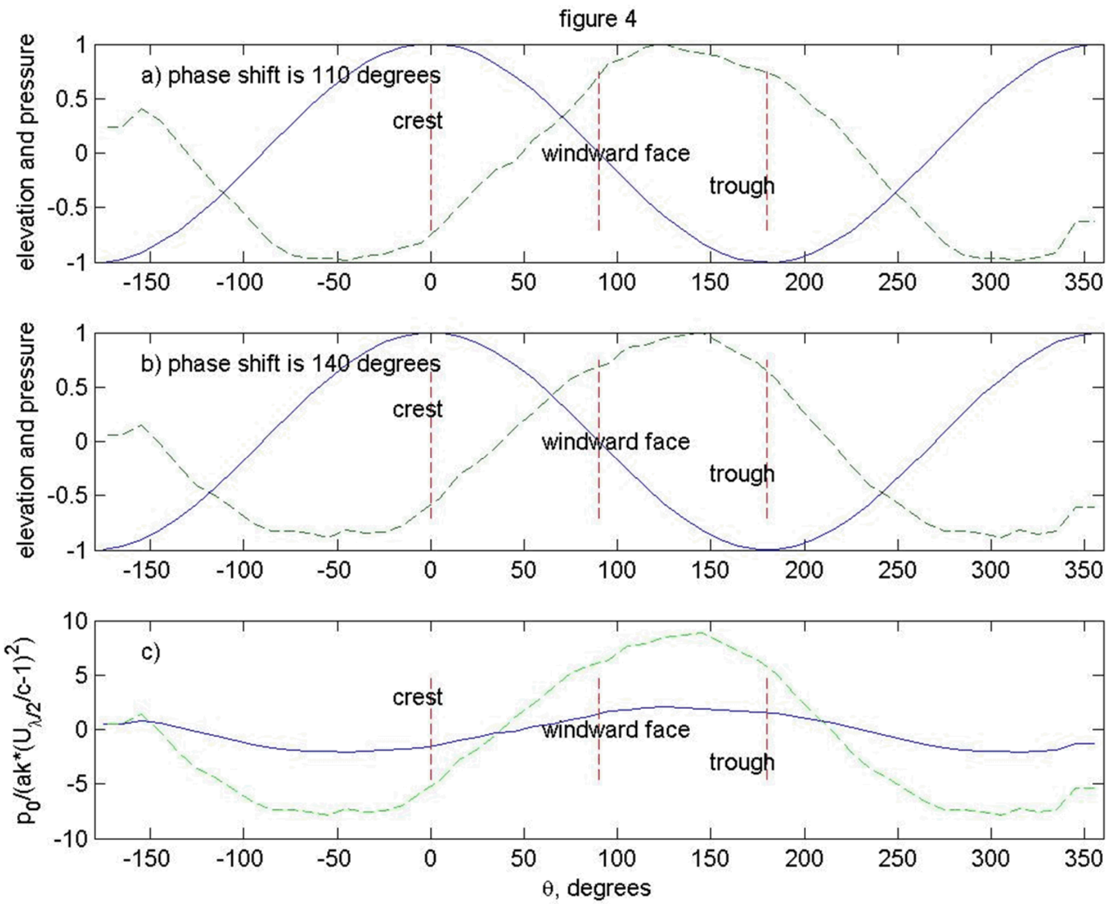

The parameterisation

$$\boxed{\frac{dE(k,f,\theta,x,t)}{dt} = S_{in} + S_{ds} + S_{nl} + S_{bf}}$$

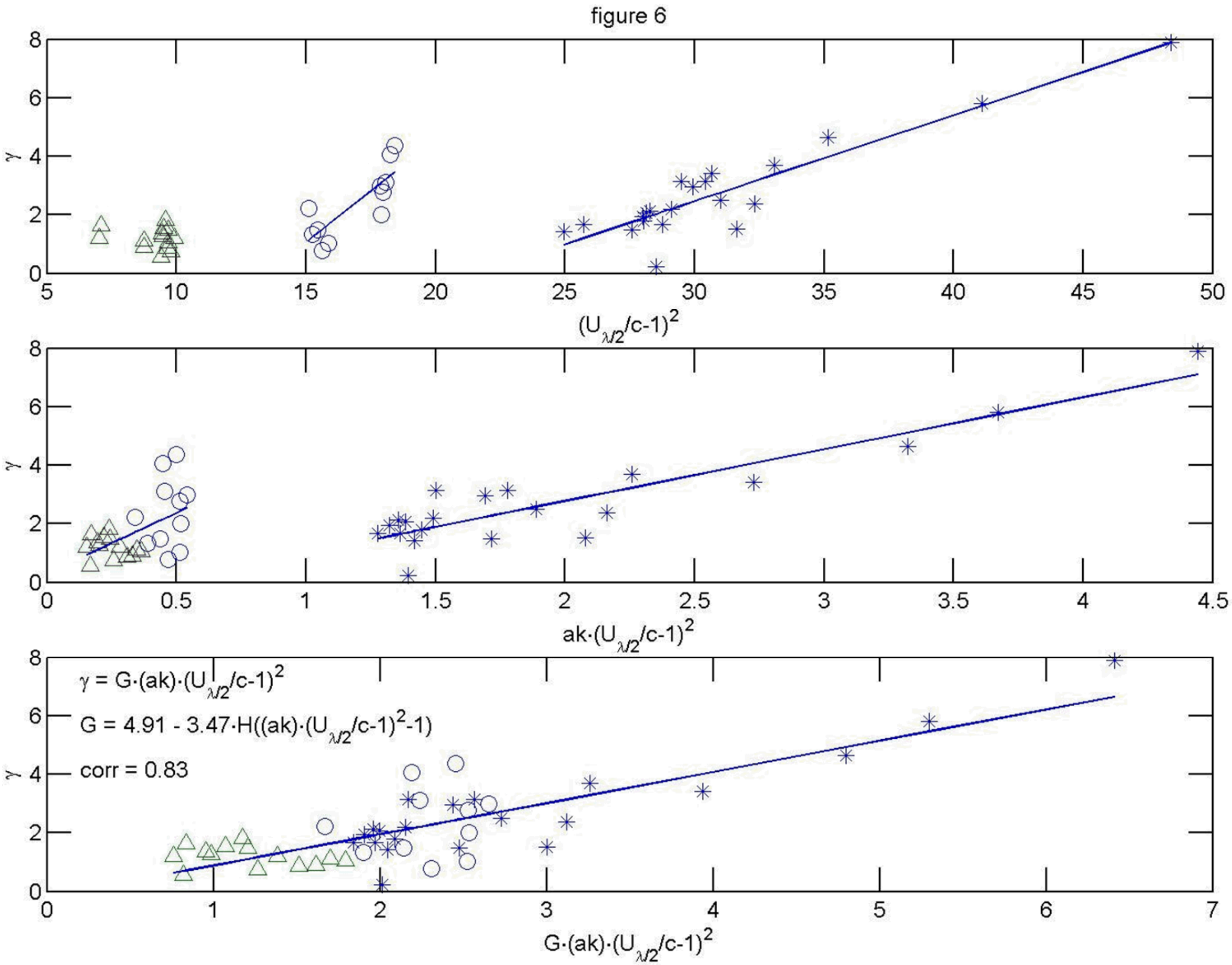

$$\frac{dE(k,f,\theta,x,t)}{dt} = S_{in} + S_{ds} + S_{nl} + S_{bf}$$

Flow separation due to breaking

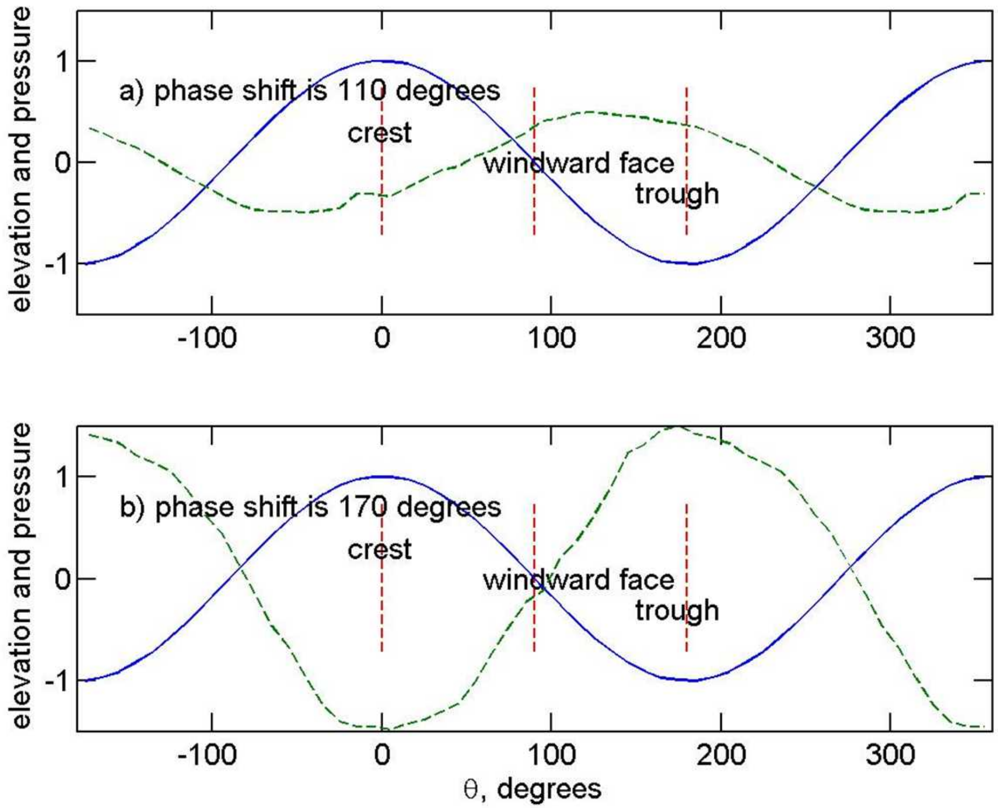

$$\gamma(f) = \gamma_0(f)(1+b_T)$$

Wind Input – S_{in}

$$\frac{dE(k,f,\theta,x,t)}{dt} = S_{in} + S_{ds} + S_{nl} + S_{bf}$$

Donelan, Babanin, Young and Banner (Part I, JTEC, 2005; Part II, JPO, 2006, Part III, JPO, 2007)

• a new parameterisation of the wind input function, based on field measurements, is suggested.

• the parameterisation includes very strongly forced and steep wave conditions, the wind input for which has never before been directly measured in field conditions.

• new physical features of air-sea exchange have been found:

- full separation of the air flow at strong wind over steep waves
- leads to the sea drag saturation
- the exchange mechanism is non-linear and depends on the wave steepness
- enhancement of the wind input over breaking waves

Breaking Dissipation S_{ds}

$$\frac{dE(k,f,\theta,x,t)}{dt} = S_{in} + S_{ds} + S_{nl} + S_{bf}$$

two passive acoustic methods to study spectral dissipation
- segmenting a record into breaking and non-breaking segments
- using acoustic signatures of individual bubble-formation events

Whitecapping Dissipation S_{ds}

$$\frac{dE(k, f, \theta, x, t)}{dt} = S_{in} + S_{ds} + S_{nl}$$

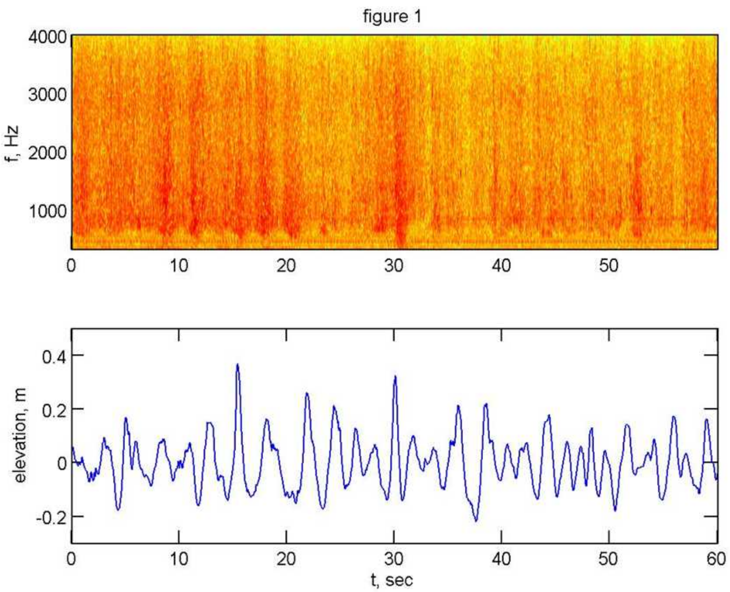

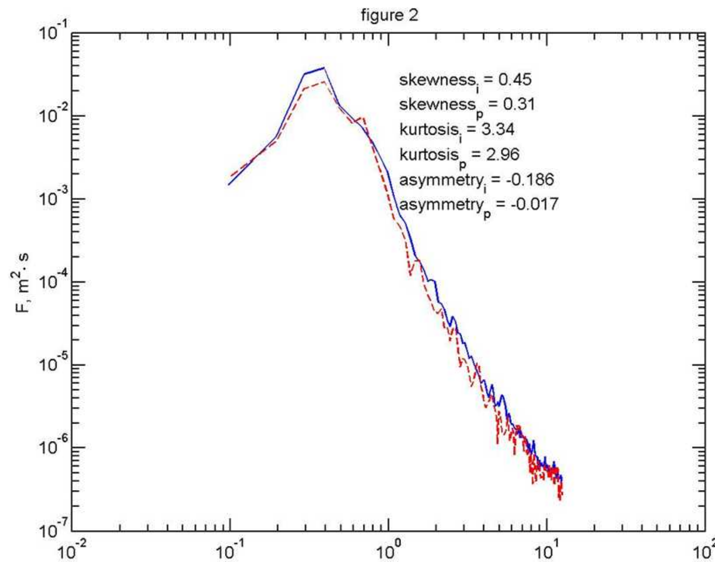

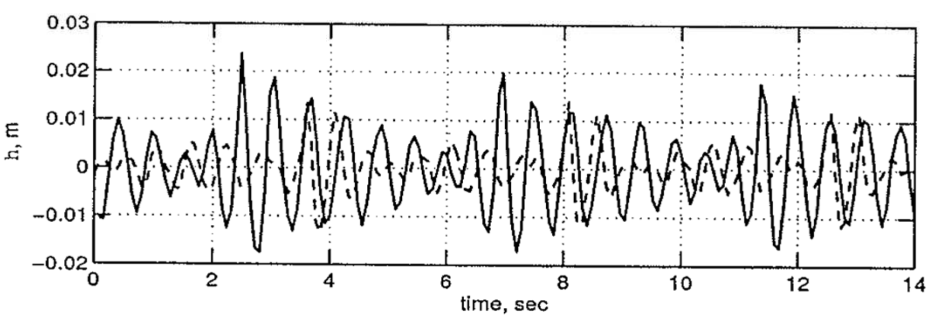

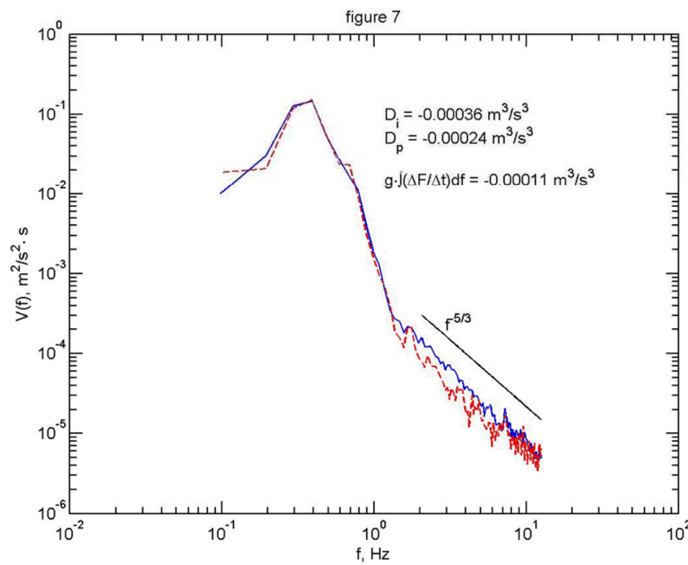

White Cap Dissipation S_{ds}

$$\boxed{\frac{dE(k,f,\theta,x,t)}{dt} = S_{in} + S_{ds} + S_{nl}}$$

1) Segmenting the record

Directional dissipation

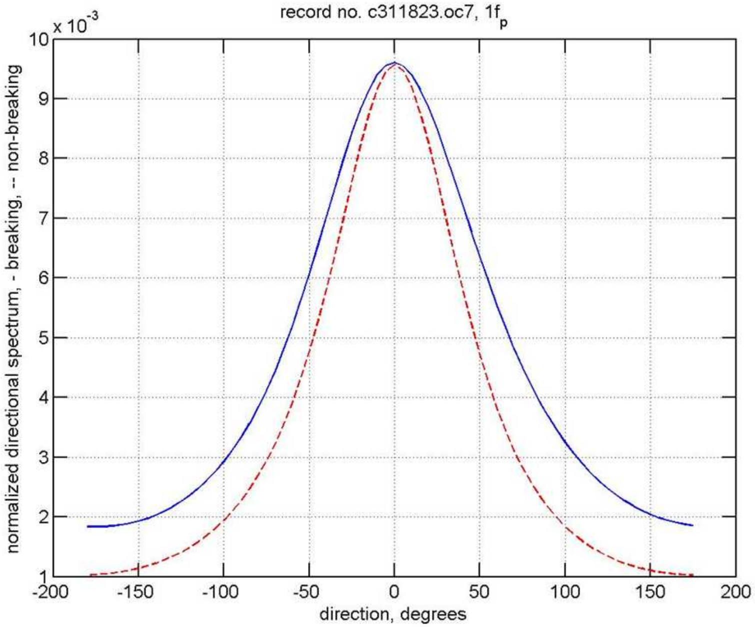

f_p

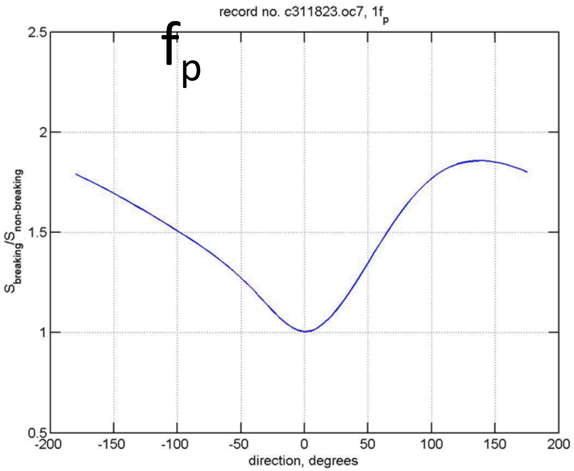

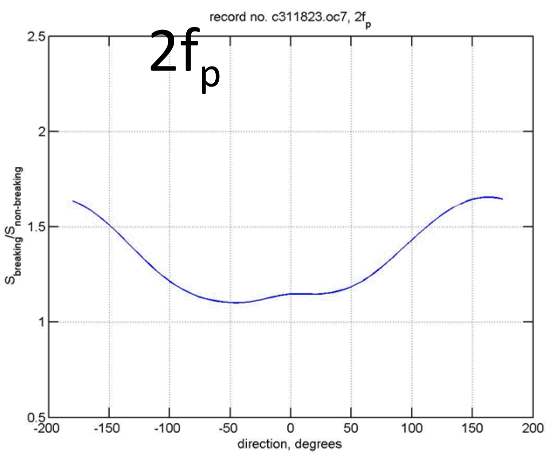

White Cap Dissipation S_{ds}

$$\frac{dE(k,f,\theta,x,t)}{dt} = S_{in} + S_{ds} + S_{nl}$$

2) Individual bubble formation
frequency distribution of breaking probability b_T

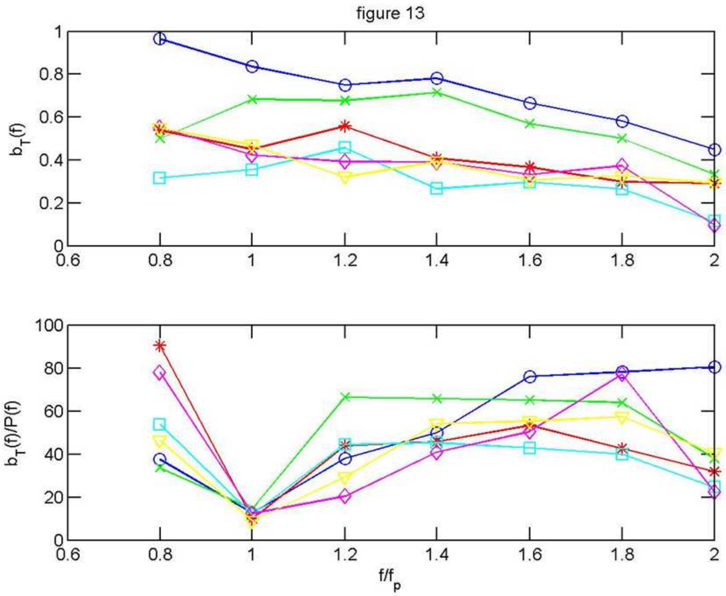

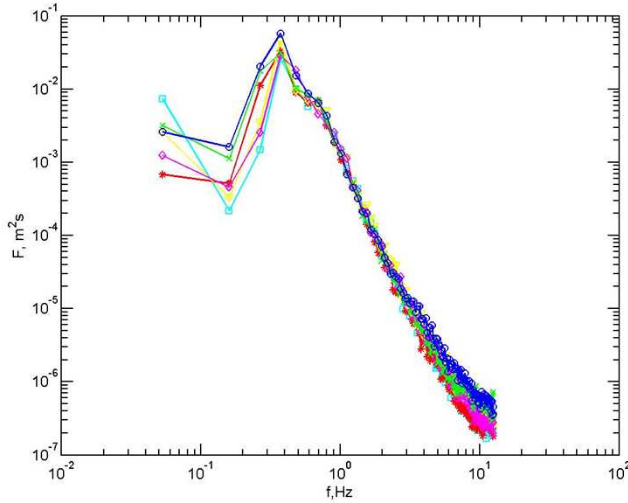

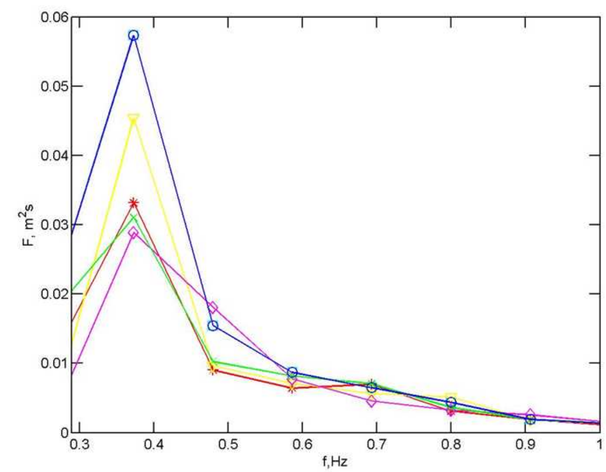

- Linear dependence at the peak
- Cumulative effect at small scales
- Direct dependence on the wind at strong forcing

White Cap Dissipation S_{ds}

$$\frac{dE(k,f,\theta,x,t)}{dt} = S_{in} + S_{ds} + S_{nl} + S_{bf}$$

- spectral dissipation was approached by two independent means based on passive acoustic methods

- if the wave energy dissipation at each frequency were due to whitecapping only, it should be a function of the excess of the spectral density above a dimensionless threshold spectral level, below which no breaking occurs at this frequency. This was found to be the case around the wave spectral peak. dominant breaking

- dissipation at a particular frequency above the peak demonstrates a cumulative effect, depending on the rates of spectral dissipation at lower frequencies

$$S_{ds}(f) = a \cdot f(F(f) - F_{thr}(f))A(f) + b\int_{f_p}^{f}(F(g) - F_{thr}(g))A(g)dg$$

- dimensionless saturation threshold value of $\sqrt{\sigma_{thr}(f)} \approx 0.035$

should be used to obtain the dimensional spectral threshold $F_{thr}(f)$ at each frequency f

- dependence on the wind at strong wind forcing

Balance of dissipation in the water column and the wind input

$$\boxed{\frac{dE(k,f,\theta,x,t)}{dt} = S_{in} + S_{ds} + S_{nl}}$$

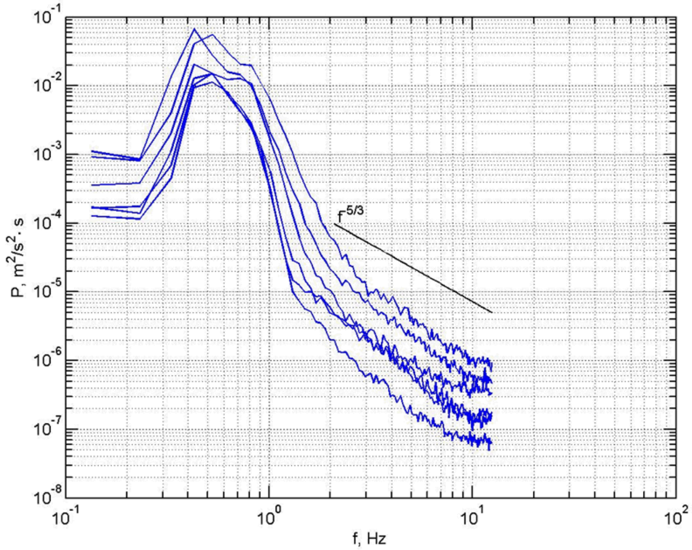

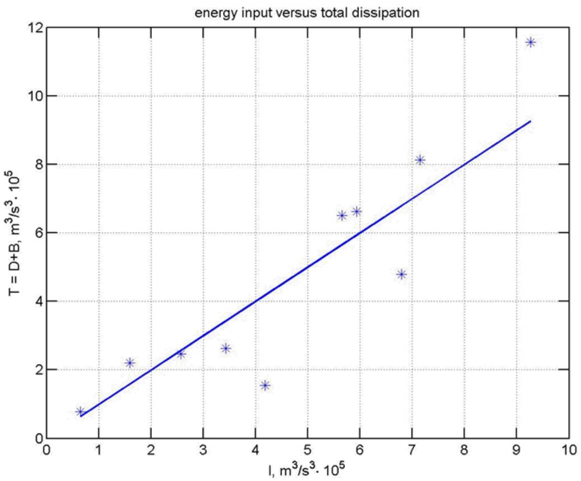

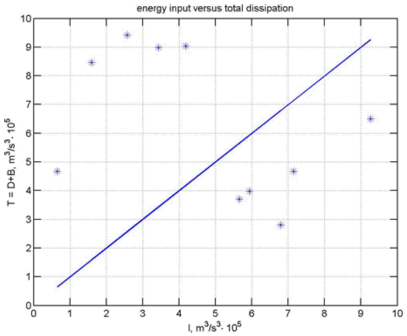

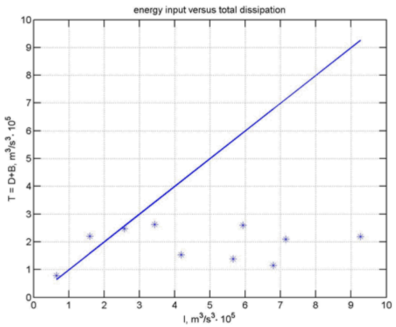

$$\varepsilon(z) = \begin{cases} const & z \le 0.4H_s \\ z^{-1} & z > 0.4H_s \quad U < 7.5 \\ z^{-2} & z > 0.4H_s \quad U \ge 7.5 \end{cases}$$

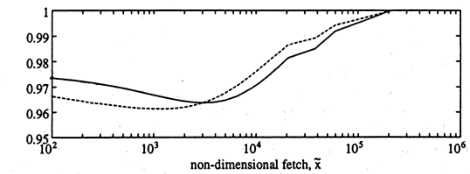

The approach

- Traditional approach (ie. Komen et al. (1984)): reproduce known growth curves – i.e. model the balance of the source functions rather than the functions themselves
- Constraint approach: following suggestion at WISE-2004 (Reading, England) by Mark Donelan
- Main constraint: integral wind momentum input must be equal to the total stress less viscous stress:

$$\int_0^{f_\infty} S_{in}^m(f)df = \int_0^{f_\infty} \frac{k}{\omega} S_{in}(f)df = \tau_w$$

- experimental dependencies for total stress and viscous stress are used
- experimental dependencies for ratio ot total input and total dissipation are used

$$\int_0^{f_\infty} S_{ds}(f)df \leq \int_0^{f_\infty} S_{in}(f)df$$

Waves and air-sea interactions

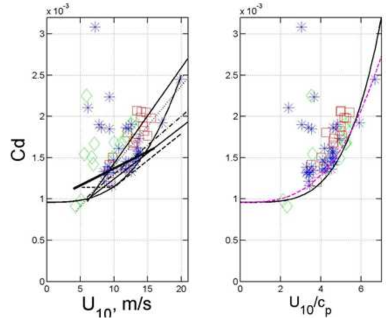

- in air-sea interaction and ocean-mixing models, the wind stress is usually parameterised to directly drive the dynamics of the upper ocean
- ~90% of the flux, however, first input into the waves
- air-sea coupling is usually parameterised in terms of the drag coefficient C_d

$$\tau = \rho_a u_*^2 = \rho_a C_d U_{10}^2$$

- the parameterisation relies on the concept of the constant flux layer
- C_d is routinely parameterised in terms of wind speed U_{10}
- scatter has not improved over some 30 years
- coupling with wave models is necessary

Gustiness

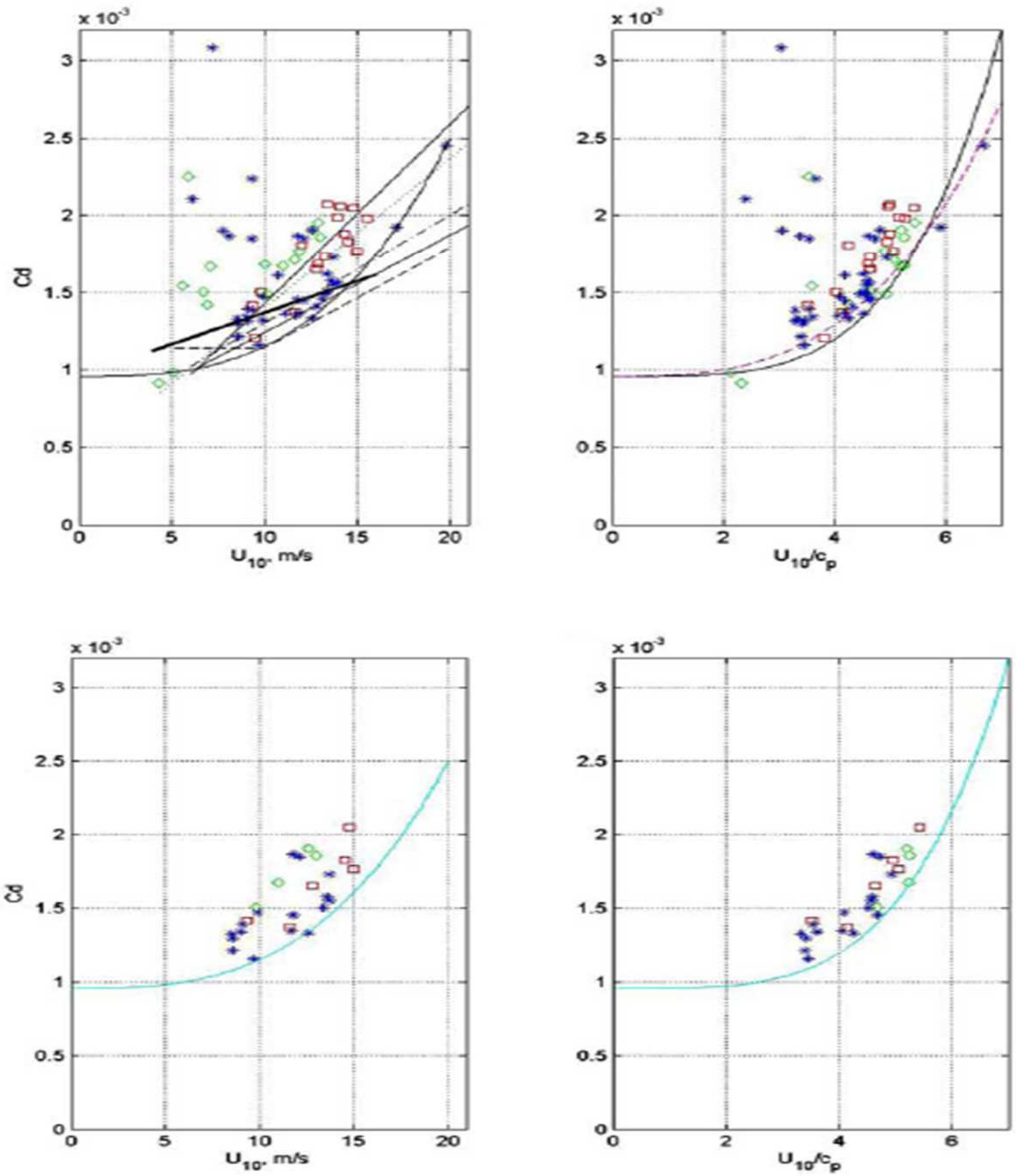

Breaking and Directional Spreading

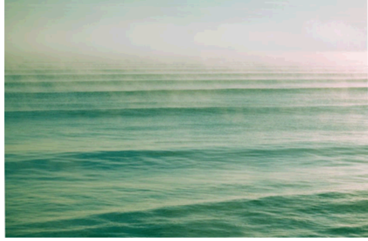

Dependence on breaking

Babanin, 2011

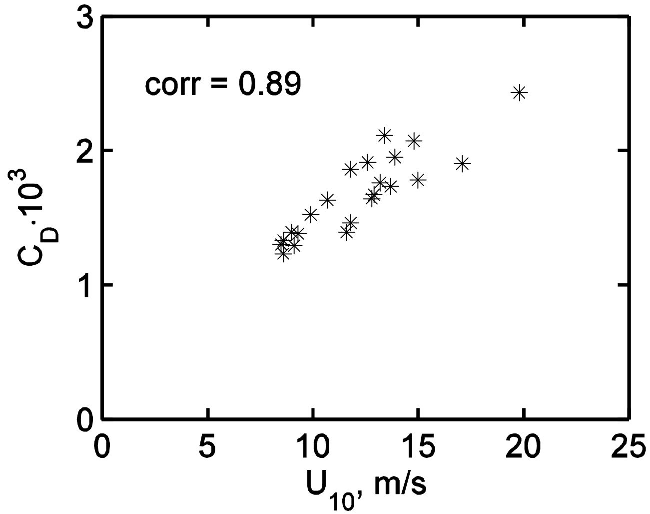

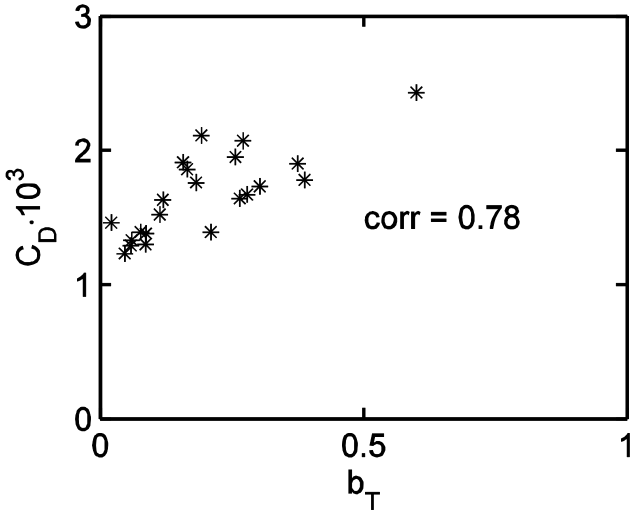

4. Result

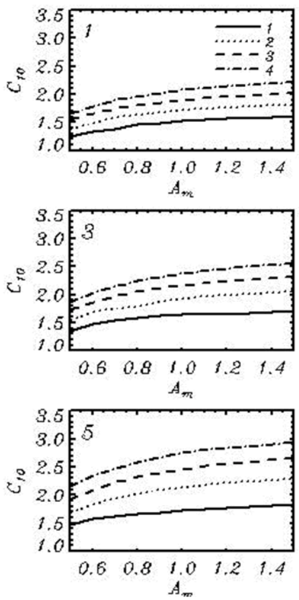

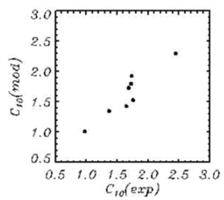

*Comparison of drag coefficient C_{10} (mod) calculated CR model with experimental data on spreading with experimental data on drag coefficient C_{10} (exp).

*Dependence of drag coefficient on angular spreading, characterized by parameter A_m. *Inverse wave age U_{10}/C_p is indicated in top left corner.*
1- U_{10}=10 m/s; 2- U_{10}=15 m/s;
3- U_{10}=20 m/s; 4- U_{10}=25 m/s

Dependence on directional spreading

Ting et al., JGR, in press

$$K(U/c_p,f,\mu)=A(U/c_p,f)\cos^{2s(U/c_p,f)}(\mu-\mu_0/2)$$

U/c_p= 1, 3, 5

Humidity

Toffoli et al., JGR, in press

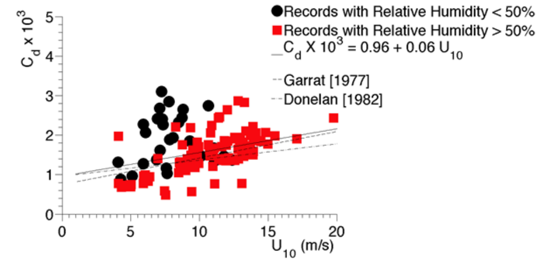

Based on Lake George data, C_D versus humidity

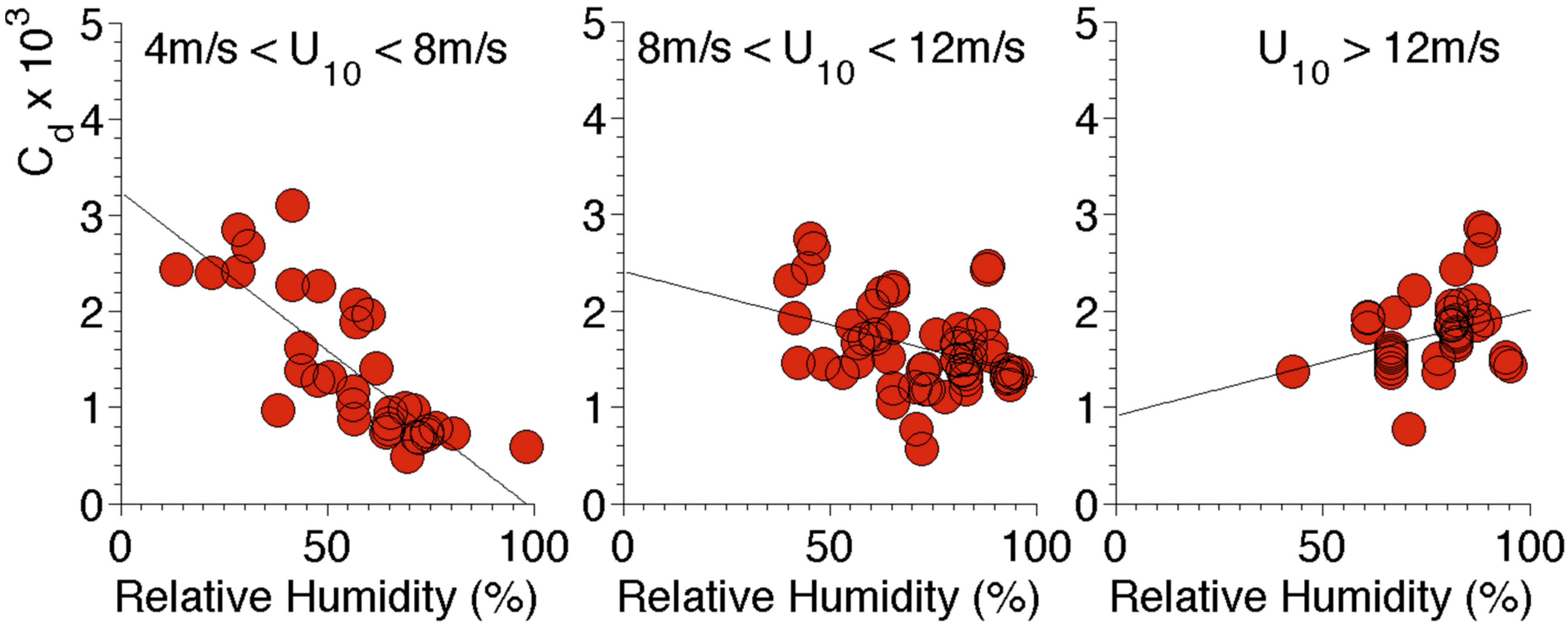

Wind Input and Wind Stress

$$\tau = \rho_a u_*^2 = \rho_a C_d U_{10}^2$$

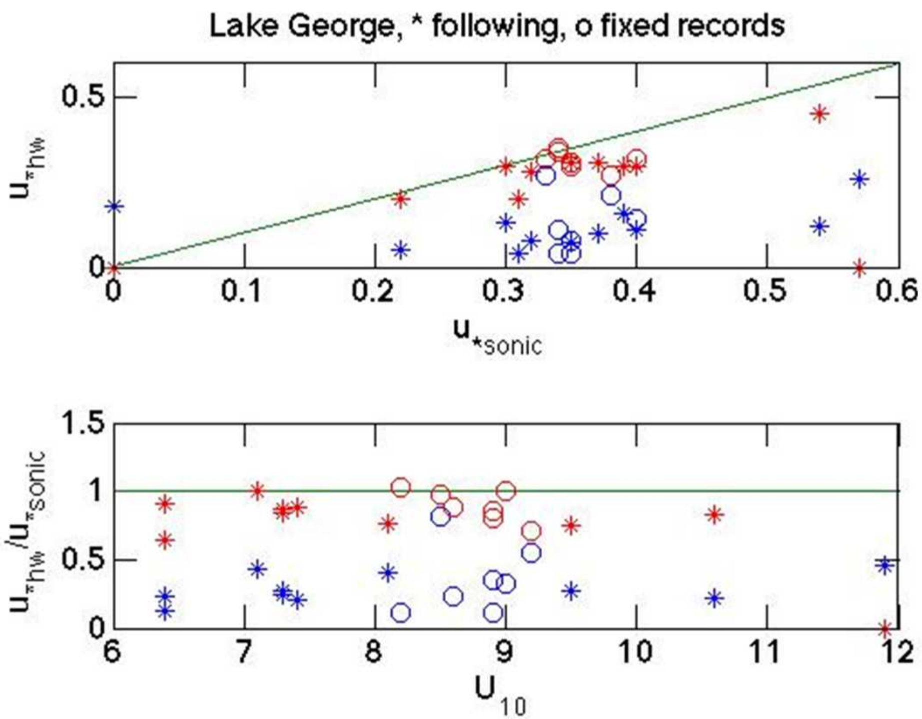

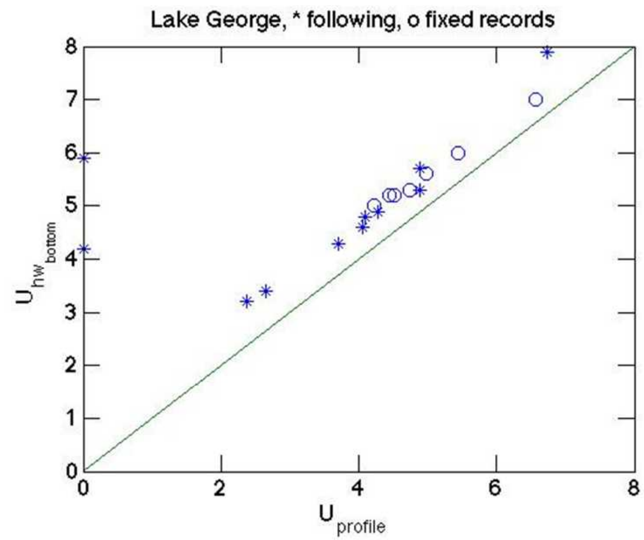

Turbulent fluxes are not constant in WBL

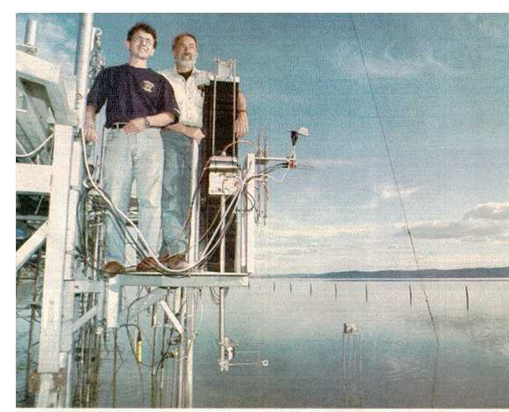

Wind: What do we need most?

- Directional distribution of the wind input
- Fluxes: momentum flux, heat flux, moisture, spray
- Surface stress versus mean wind speed elevated
- Advanced sea-drag parameterisations

White Cap Dissipation S_{ds}

$$\frac{dE(k,f,\theta,x,t)}{dt} = S_{in} + S_{ds} + S_{nl}$$

2) Individual bubble formation

bubble size is related to the breaking severity

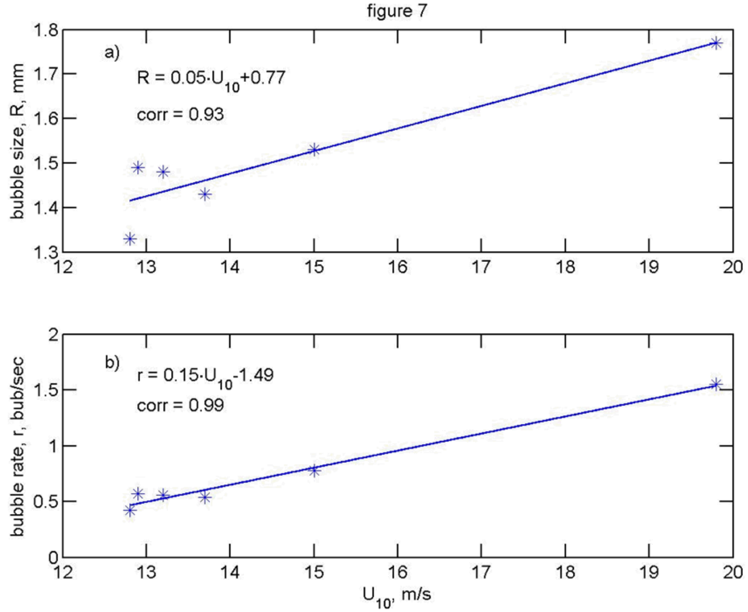

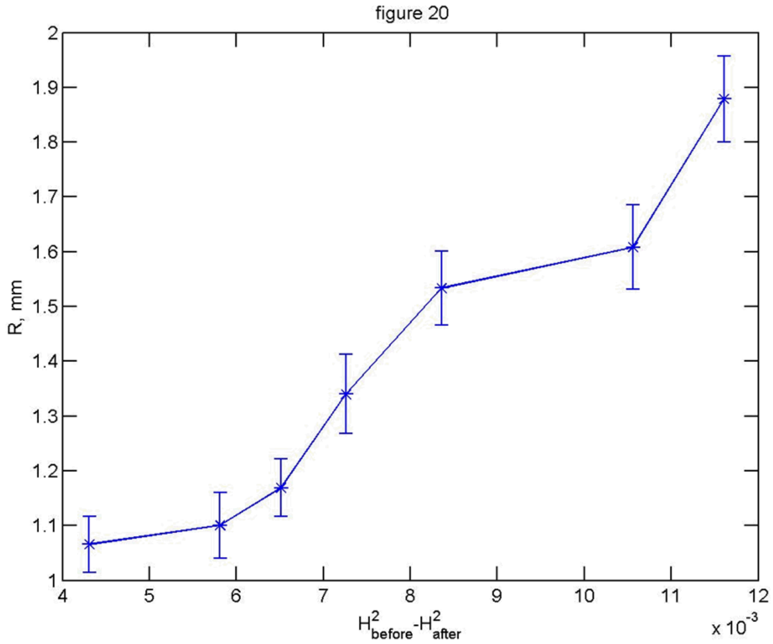

Dissipation: what do we need most?

- More direct measurements of the dissipation rates across the spectrum
- Measurements and parameterisation of the breaking severity
- Whitecapping coverage versus breaking severity
- Dependence of the whitecapping coveraged environmental properties, i.e. wind, wave age, surface temperature, biological surfactants etc.
- Directional distribution of the dissipation

Air-sea interactions at extreme wind forcing

- At wind speeds

$$U>32m/s$$

dynamics of the atmospheric boundary layer, of the ocean wave surface and of the upper ocean layer – all change

- Strong correlation of wave asymmetry A_s with wind forcing, asymmetry saturates (Leikin et al., 1995, NPG) at

$$U_{10}\sim 34m/s$$

Change of the wave breaking mechanism to, perhaps, breaking due to direct wind forcing

- Drag saturates (Powel et al., 2003, Nature) at

$$U_{10}=32\text{-}33m/s$$

- additional mechanism of air injection due to bubbles of 1mm diameter transported down to 20m below the surface and dissolved due to the hydrostatic compression (McNeil & D'Asaro, 2007, J. Mar. Scie.) at

$$U_{10}>35m/s$$

Tropical Cyclone Yasi – setup & observations

wave data

wind data

best track

altimeter tracks

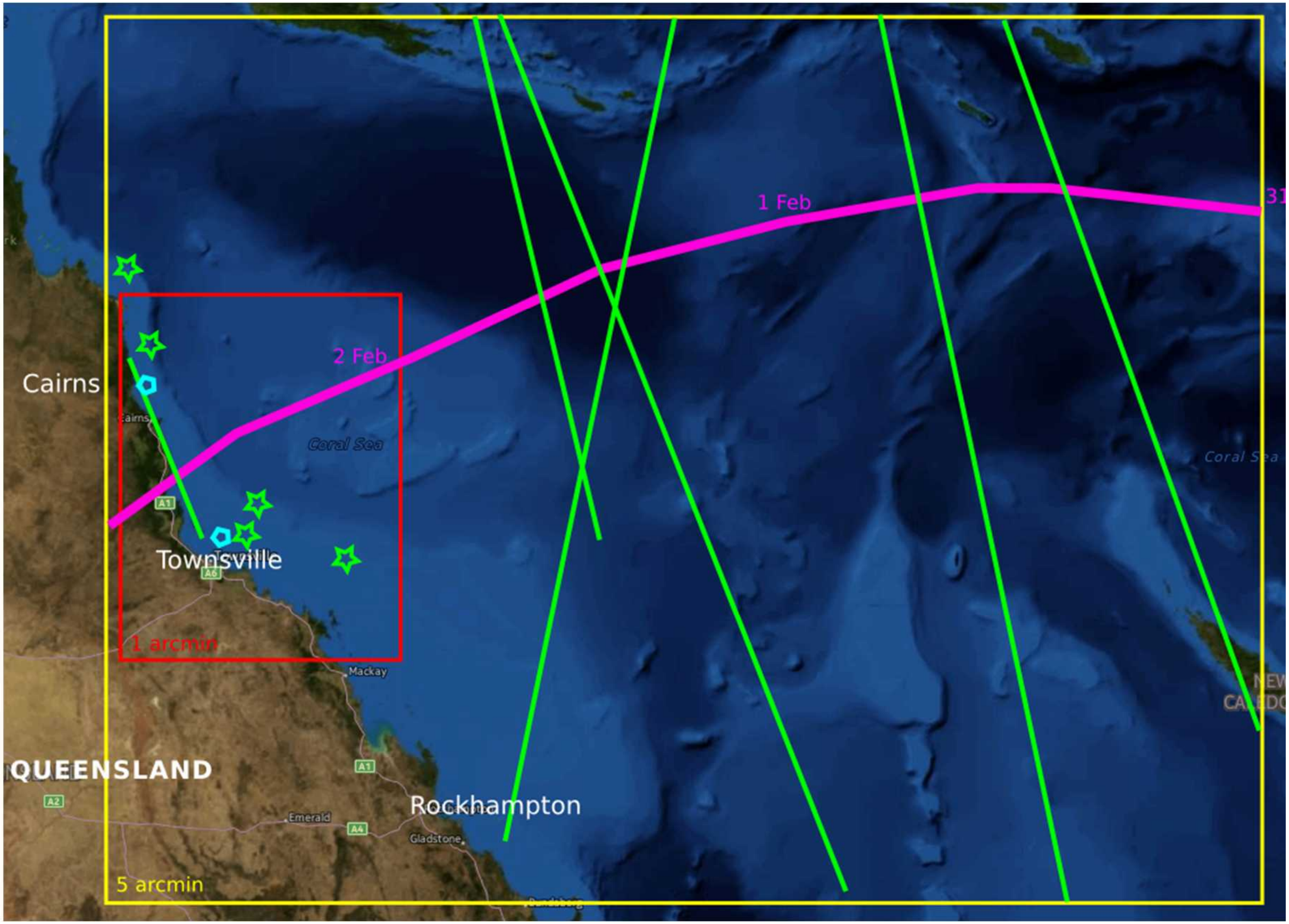

1600x2000km

Yasi – along-track comparison

- deep water track: ENVISAT – 1 Feb 23:36 UTC
- winds (top) and wave height (bottom)

Yasi – in situ waves

- observed waves next to Townsville (ADCP) and Cape Cleveland (DERM) for all three wind fields

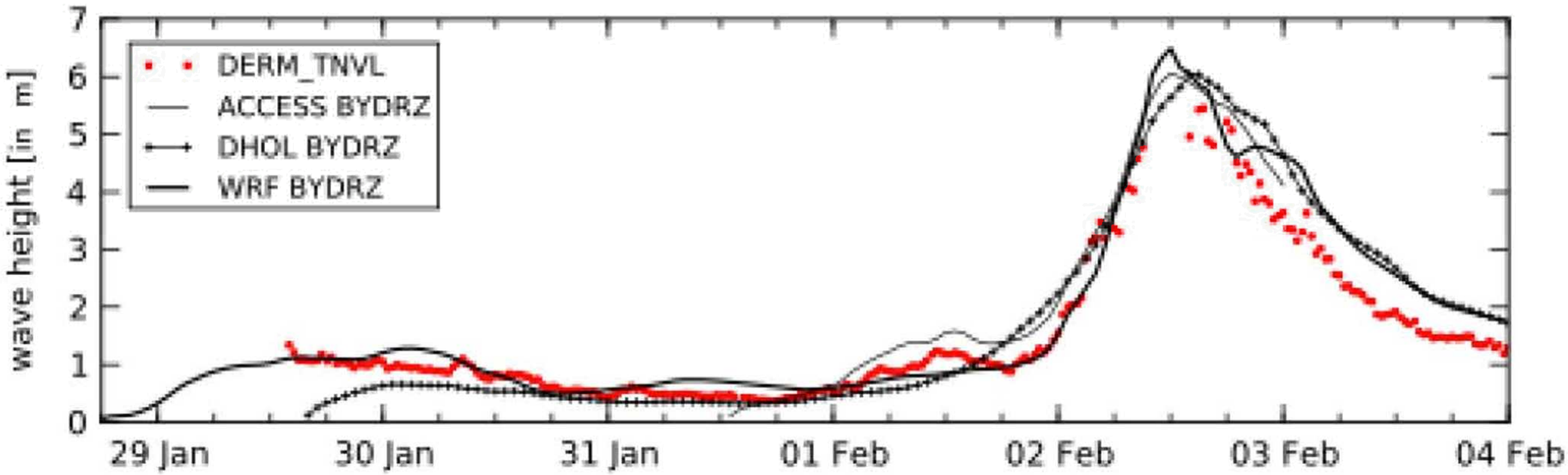

Babanin, A.V., T.-W. Hsu, A. Roland, S.-H. Ou, D.-J. Doong, and Y.-M. Fan, 2010: Spectral modelling of Typhoon Krosa, *Natural Hazards and Earth System Sciences*, 2011

- highest ever waves are measured off the coast of Taiwan
- spectral models cannot reproduce them
- the only property the wave height responds in the models – is the bottom-induced breaking formulation

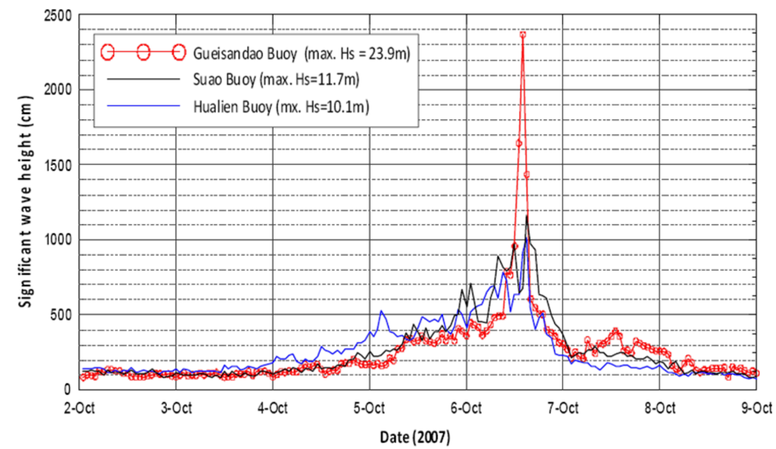

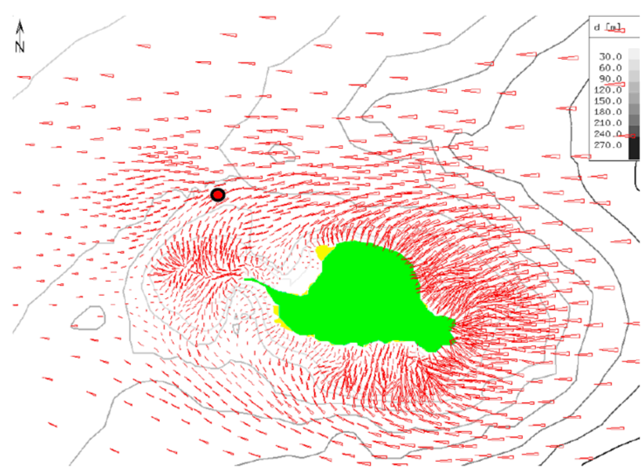

What we need

- At wind speeds

$$U>32m/s$$

dynamics of the atmospheric boundary layer, of the ocean wave surface and of the upper ocean layer – all change

- Details are vague, physics is unknown
- Any field observations are helpful: fluxes, sea drag, wave spectra and wave statistics, whitecapping and dissipation, bottom-induced breaking of extreme waves

Swell attenuation due to wave turbulence

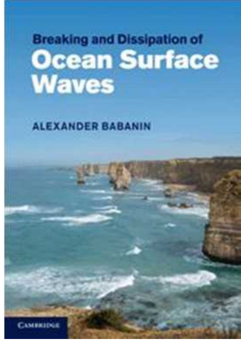

$$\varepsilon = 300 \cdot a^{3.0 \pm 1.0} \quad b = b_1 k \omega^3 = 30. \quad b_1 = 0.004$$

Dissipation

- volumetric

$$\epsilon_{dis} = b_1 k \omega^3 a_0^3 = 0.004 k u_{orb}^3.$$

- per unit of surface

$$D_a = b_1 k \int_0^\infty u(z)^3 dz = b_1 k u_0 \int_0^\infty \exp(-3kz) dz = \frac{b_1}{3} u_0^3.$$

- per unit of propagation distance

$$D_x = \frac{1}{c_g} D_a = \frac{b_1}{3} 2 \frac{k}{\omega} u_0^3 = \frac{2}{3} b_1 k \omega^2 a_0^3 = \frac{2}{3} b_1 g k^2 a_0^3.$$

$$\frac{g}{2} \frac{\partial (a_0(x)^2)}{\partial x} = \frac{2}{3} b_1 g k^2 a_0(x)^3,$$

$$a_0(x)^2 = \frac{4}{B^2} x^{-2} = \frac{9}{4 \cdot b_1^2 k^4} x^{-2} = \frac{9}{64} 10^6 k^{-4} x^{-2}.$$

Swell attenuation due to wave turbulence

b_1=0.004

asterisks

b_1=0.002

circles

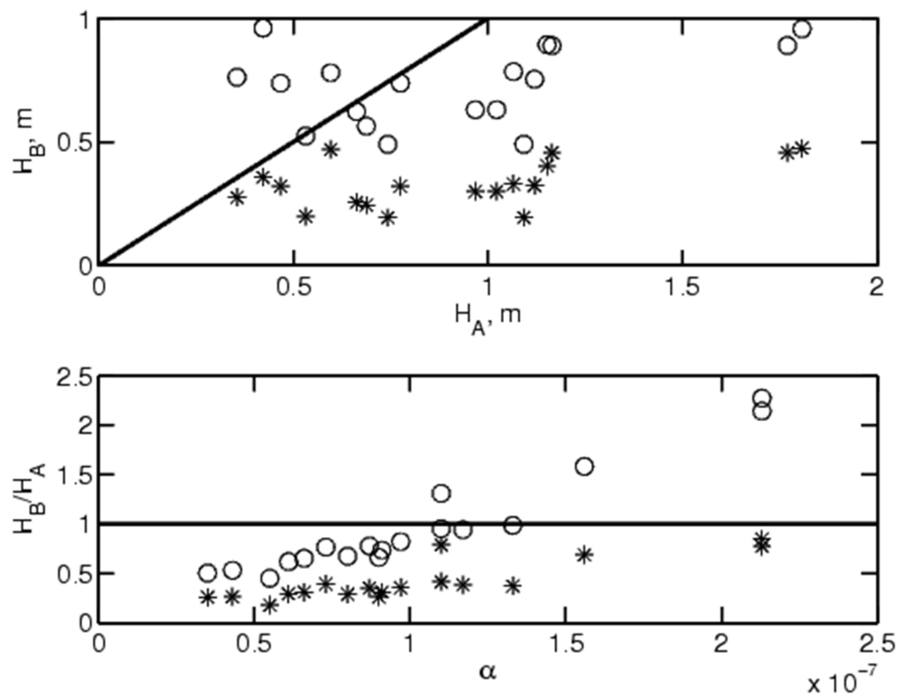

Figure 7.26 (top) Swell height H_B (7.94), estimated by means of decay described by (7.92), versus height H_A (7.95) based on the experimental decay rate α (7.60) of Ardhuin *et al.* (2009); (bottom) Ratio H_B/H_A versus α. In both subplots, asterisks correspond to the empirical coefficient (7.84) and circles to (7.96), and solid line indicates one-to-one ratio

Wind/Wave Climate

SWINBURNE UNIVERSITY OF TECHNOLOGY

Wind and waves as climate indicators

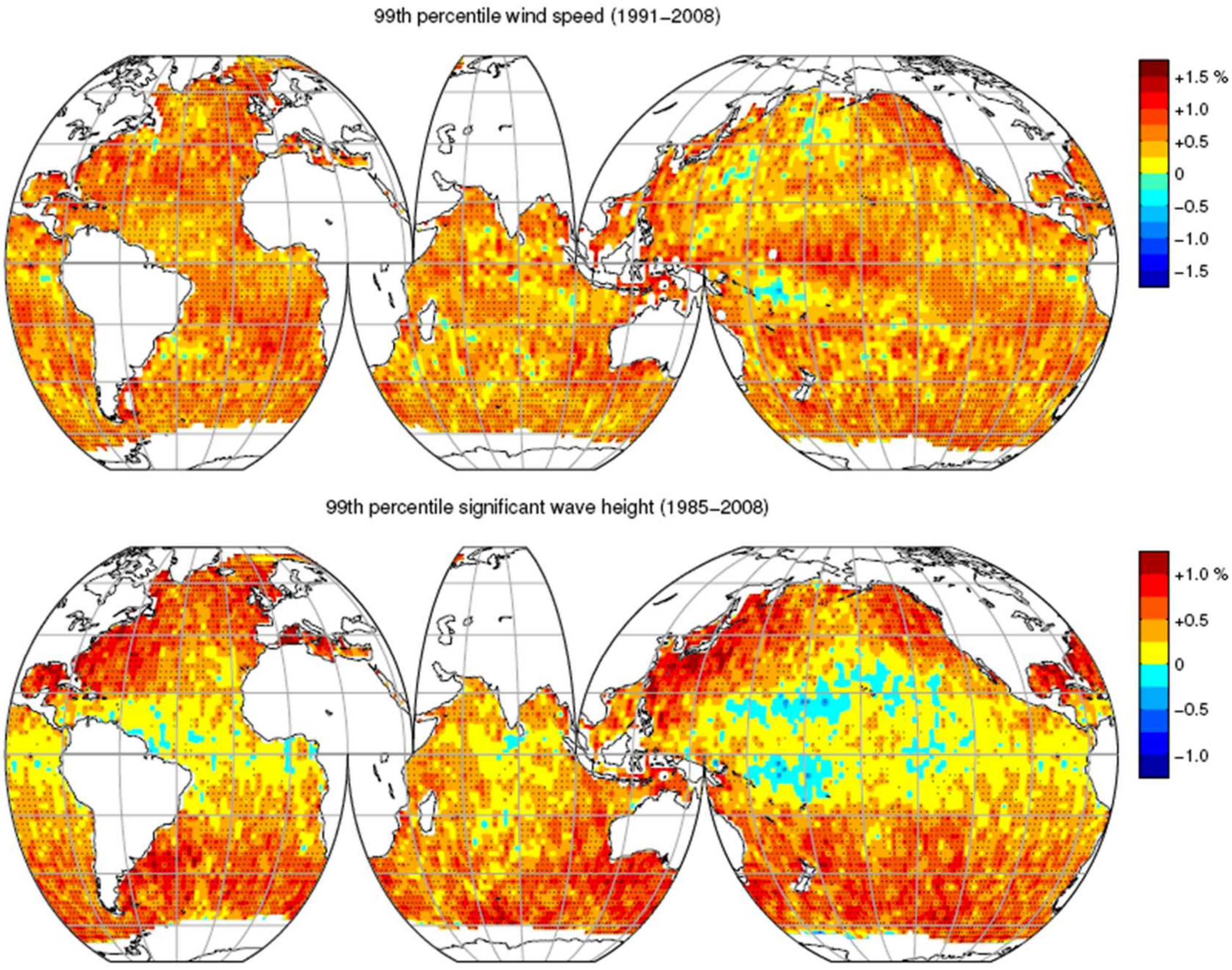

Young et al., Science, 2011

Wind Trends, by SSM/I

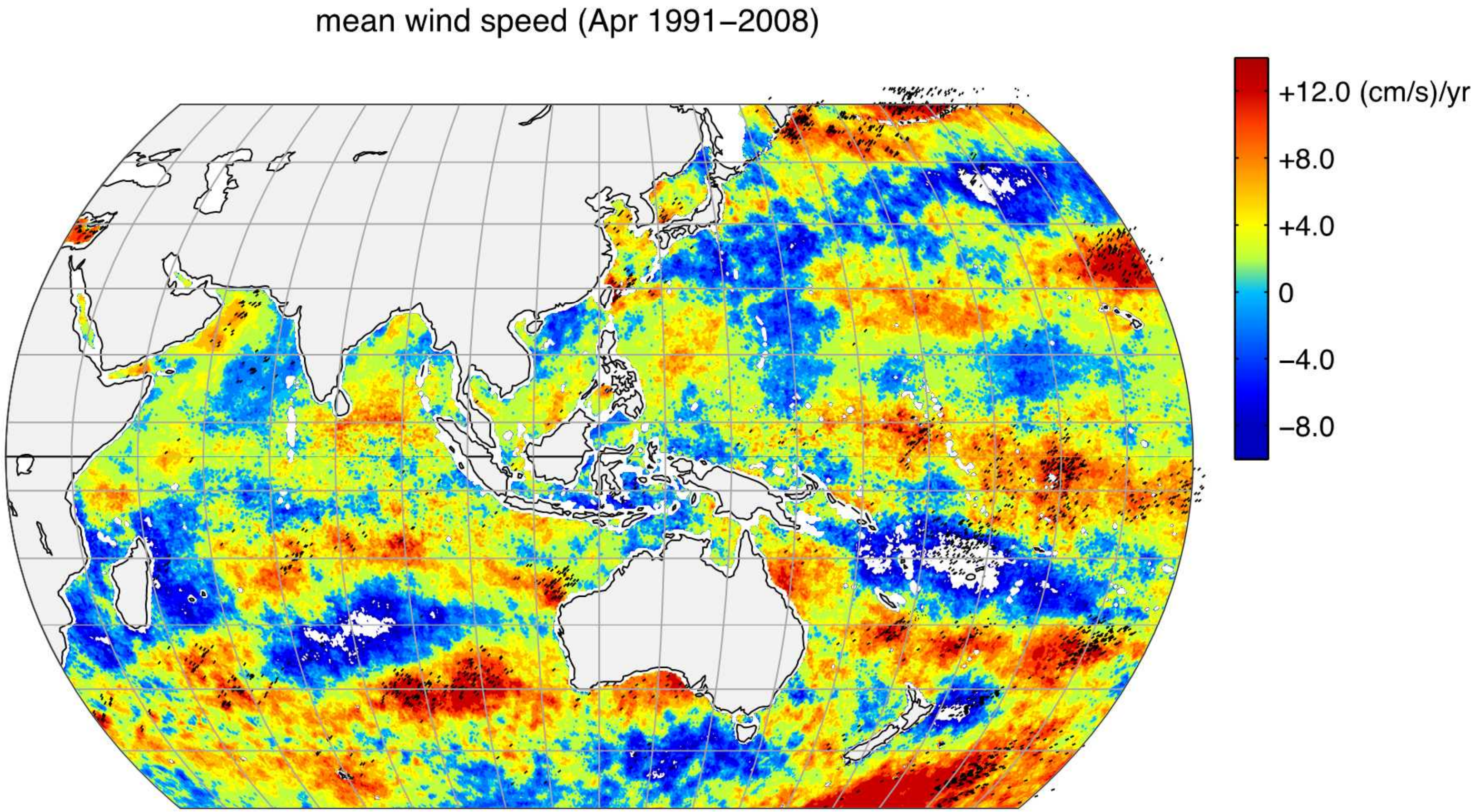

Trend analysis (MK test) applied to monthly mean SSM/I (F10,F11,F13) wind and precipitation from 1991 to 2008. Hatching indicates significant changes (normcdf test [95% level]) and contour interval is 2.00 cm s^{-1} per year.

Wind Trends, by SSM/I

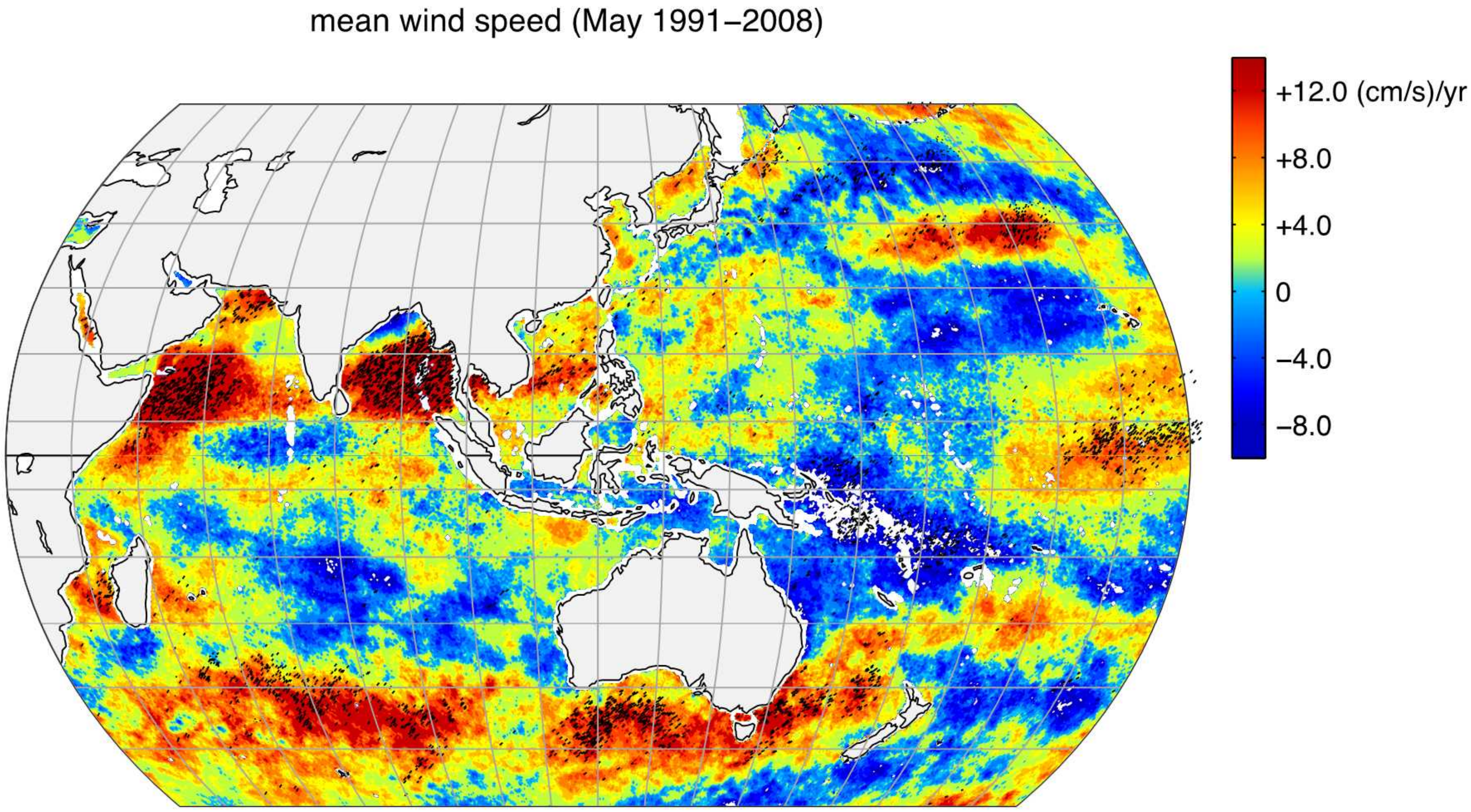

Trend analysis (MK test) applied to monthly mean SSM/I (F10,F11,F13) wind and precipitation from 1991 to 2008. Hatching indicates significant changes (normcdf test [95% level]) and contour interval is 2.00 cm s^{-1} per year.

Wind Trends, by SSM/I

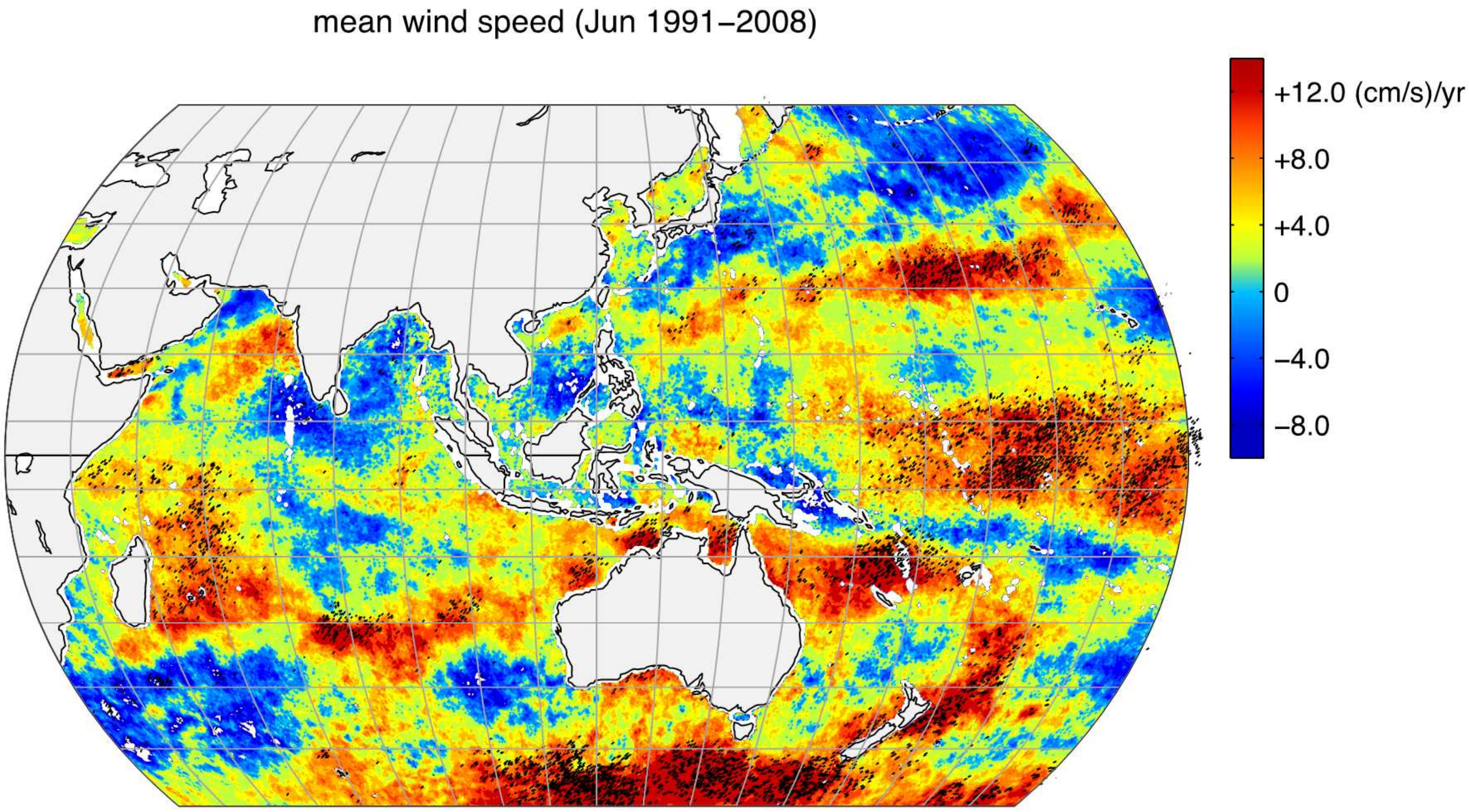

Trend analysis (MK test) applied to monthly mean SSM/I (F10,F11,F13) wind and precipitation from 1991 to 2008. Hatching indicates significant changes (normcdf test [95% level]) and contour interval is 2.00 cm s^{-1} per year.

Summary

- wave physics, what is needed
  - perhaps, 4 physics: swell, light winds, moderate winds, extreme
  - long-term observations, statistics, e.g. freak waves
  - wind stress, sea drag, fluxes across interface
  - wave dissipation, including swell, interaction with bottom, currents
  - directional distributions of energy sources/sinks
  - extreme conditions, tropical cyclones
- waves provide feedback
  - to the atmospheric boundary layer
  - to the upper ocean (usually overlooked)
  - to the large-scale air-sea interactions
  - to weather, ocean circulation and climate
- Wave/wind climate also changes
- waves can serve as a climate indicator, gradual and non-uniform

Bedforms: Sand Ripples

- Numerical Modelling
- Sediment Mobility
- **Roughness – Bedforms & Sediment Grain Size**
- Sediment Suspension
- Sediment Transport
- Conclusions

- Ripples can occur under certain conditions that are determined by Nielsen (1992)
- Ripples create a higher friction coefficient
- Can be determined empirically by using the following parameters:
  - Orbital Velocity at seabed
  - Excursion amplitude at seabed
  - Grain Size
  - Specific Gravity

Accuracy – Time Series & Scatter Plot

Significant Wave Height (Green = Observed Data, Blue = Modeled Data)

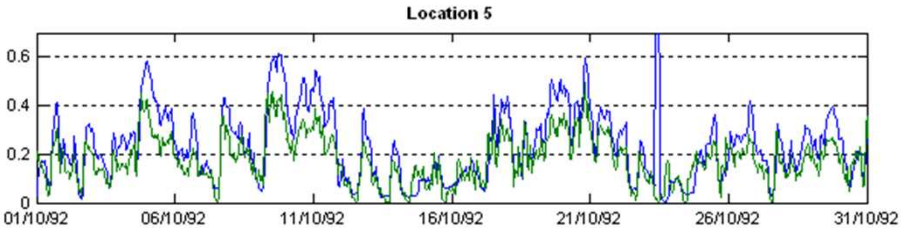

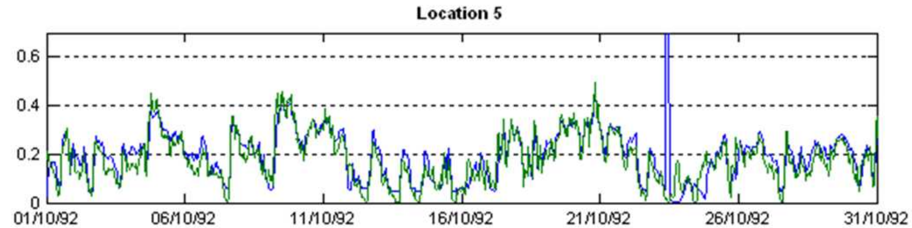

Swan Output

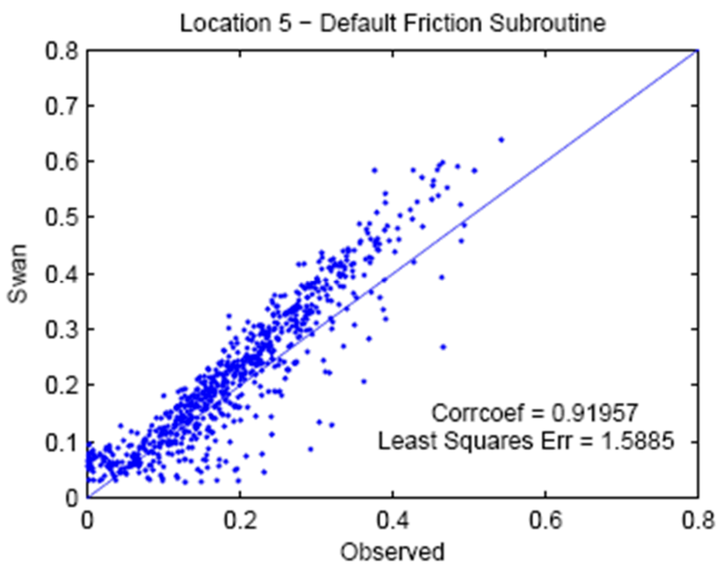

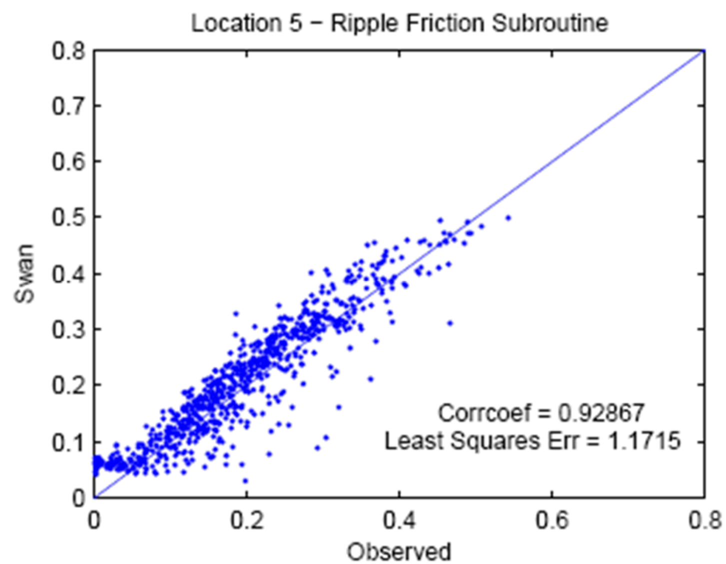

Observed Data

What if ripples don’t occur?

- Numerical Modelling
- Sediment Mobility
- **Roughness – Bedforms & Sediment Grain Size**
- Sediment Suspension
- Sediment Transport
- Conclusions

- No ripples occur when conditions too low in energy (seabed isn’t mobile)
- Ripples get washed out during large storm events
- Roughness dependent on grain size only
- Test case: Lakes Entrance, Lake George

Conclusions

- The SWAN wave model was modified to include an additional friction routine to evaluate roughness due to ripples.
- Increased dissipation due to bottom friction from ripple bedforms had a positive effect on the accuracy of modelling shallow depths with the existence of ripples.
- Roughness due to grain size also provided an acceptable roughness coefficient in the absence of ripples.

Motivation

Propagation of waves through spatially and temporally variable currents is a frequent occurrence in coastal areas

Port Phillip, Australia

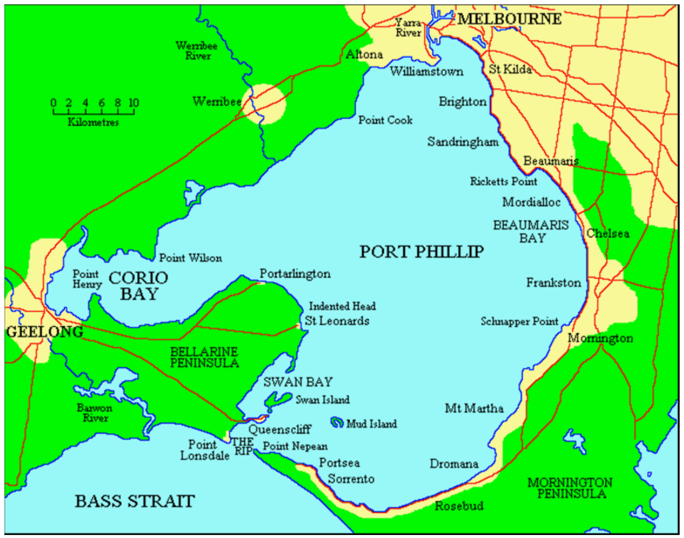

navigation

Wadden Sea, Holland

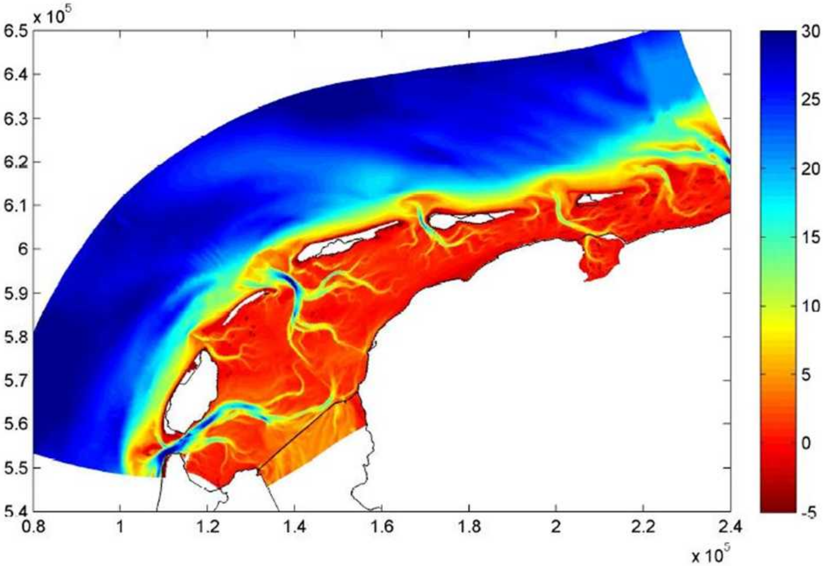

coastal defense

Waves on currents is perhaps the last loose physics in wave forecast models

Measurements, adverse currents

stronger velocity gradients, $U>c_g/4$

gradual irreversible downshift

beyond lower sideband

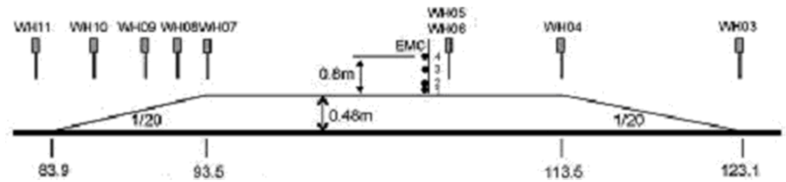

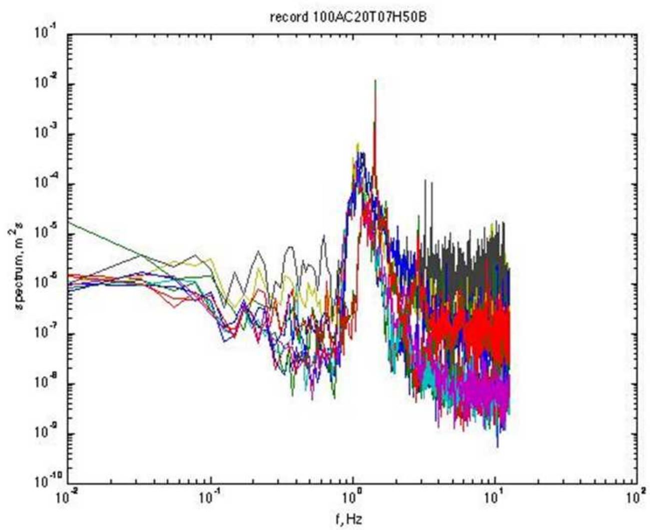

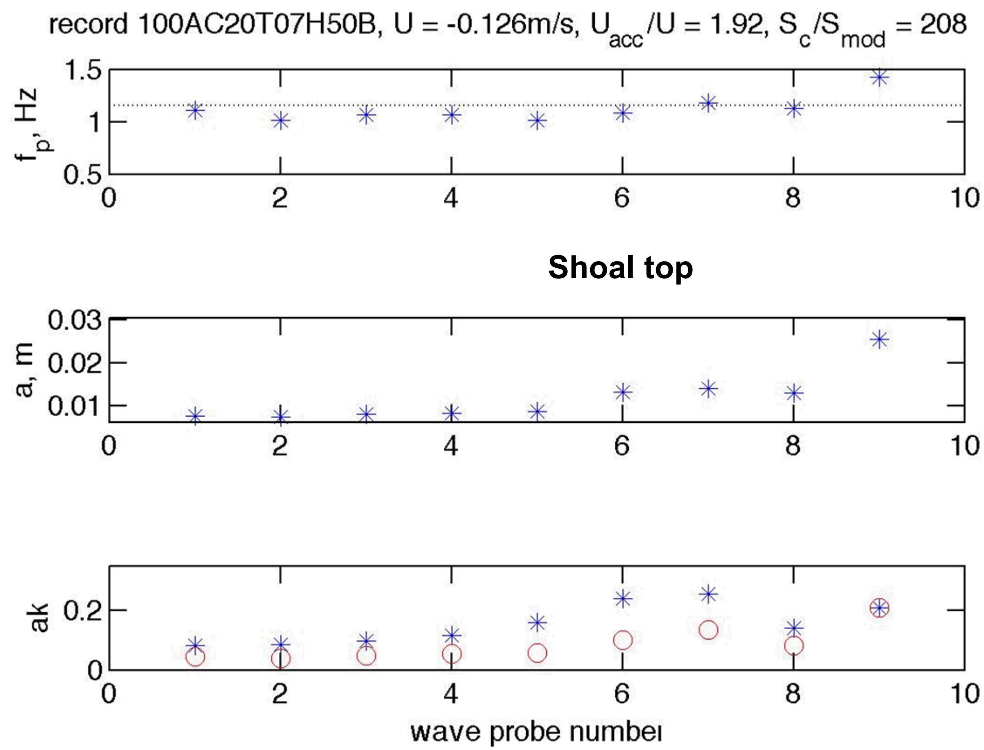

- waves propagate from right to left
- circles signify downshifting observed, dashed line the sideband
- probes 7-5 are over the bottom elevation

Young, I.R., Babanin, A.V., Stiassnie, M.A., Greenslade, D.J. (Australian Bureau of Meteorology), "Numerical modelling of extreme waves generated by tropical cyclones", Australian Research Council, Discovery Grant, 2010-2012

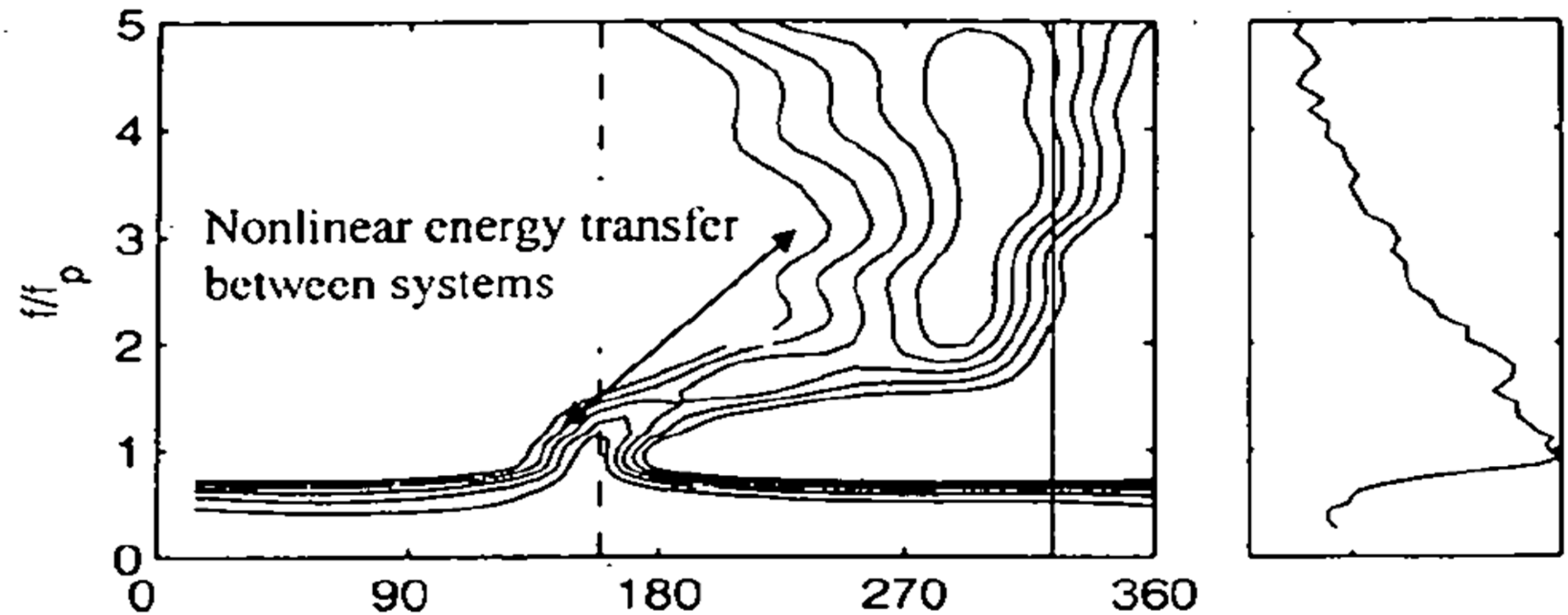

Young, 2006, *J. Geophys. Res.*

$$\frac{DE(\omega, k, \theta, \underline{x}, t)}{Dt} = S_{in} + S_{nl} + S_{ds} + \cdots$$

new S_{nl} term is to be developed

Dissipation S_{ds}

$$\frac{dE(k,f,\theta,x,t)}{dt} = S_{in} + S_{ds} + S_{nl}$$

➢ The induced dissipation can be caused by forced breaking of shorter waves due to the dominant breaking, or modulation of short waves by longer waves, or by enhanced turbulent viscosity due to the dominant breaking, or both.

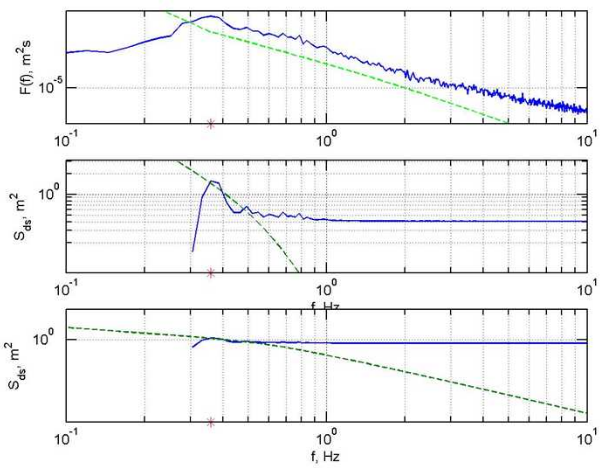

➢ importance of the cumulative dissipation is evident

$$S_{ds}(f) = a \cdot f\,(F(f) - F_{thr}(f))A(f) + b\int_{f_p}^{f}(F(g) - F_{thr}(g))A(g)dg$$

Cyclone Wave Modelling

- Change of the physical regime at extreme winds
- Cyclone Yasi
- Typhoon Krosa

Saturation of Sea Drag

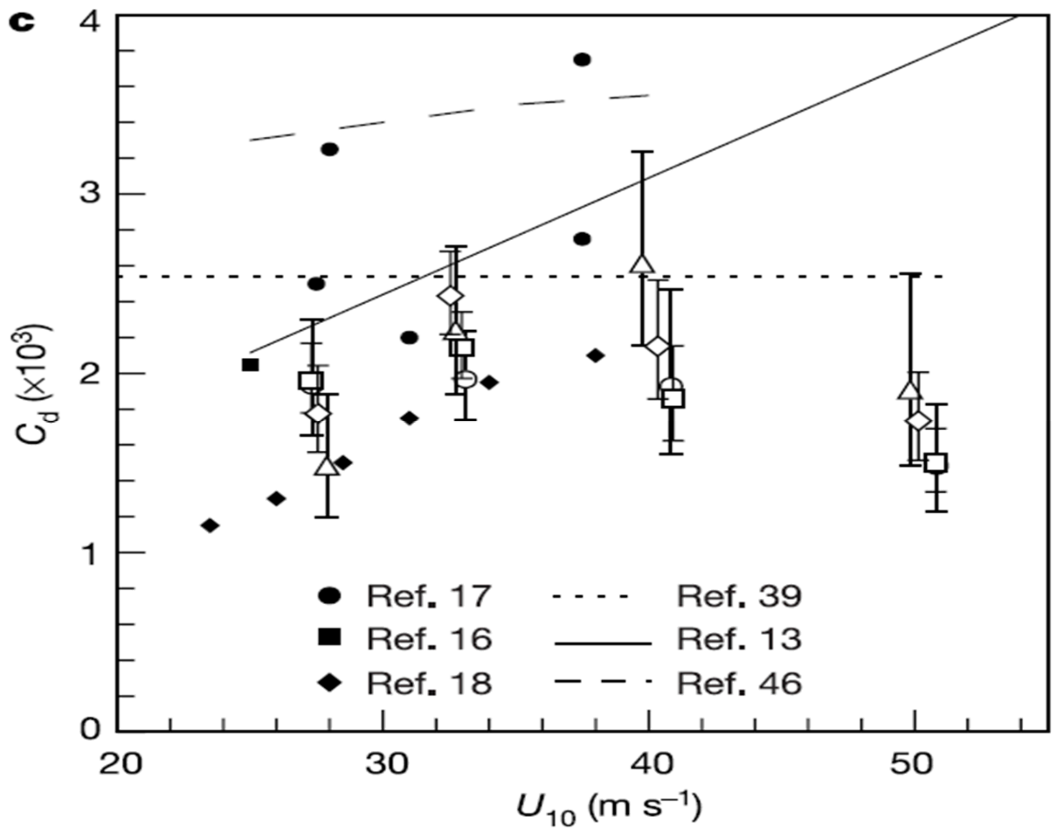

Powel et al., 2003, Nature

- Extensive research field since 2003, dozens of papers
- field and laboratory experiments
- theories:

- spray theories, 4 classes

- hydrodynamic theories, 2 classes

- instability of ripples (KH and modulatinal)

-turbulence theory: 2D turbulence suppresses 3D vortexes

- combination of those

Drag saturates at

U_{10}=32-33m/s

Shats, M., Babanin, A.V., Marusic, I., Young, I.R., Punzmann, H., Xia, H, Toffoli, A., Chalikov, D., Klewicki, J., Hutchings, N., Monti, J., “Wind profiler network for planetary boundary layer research”, , Australian Research Council, Large Equipment and Infrastructure Facilities Grant, 2012

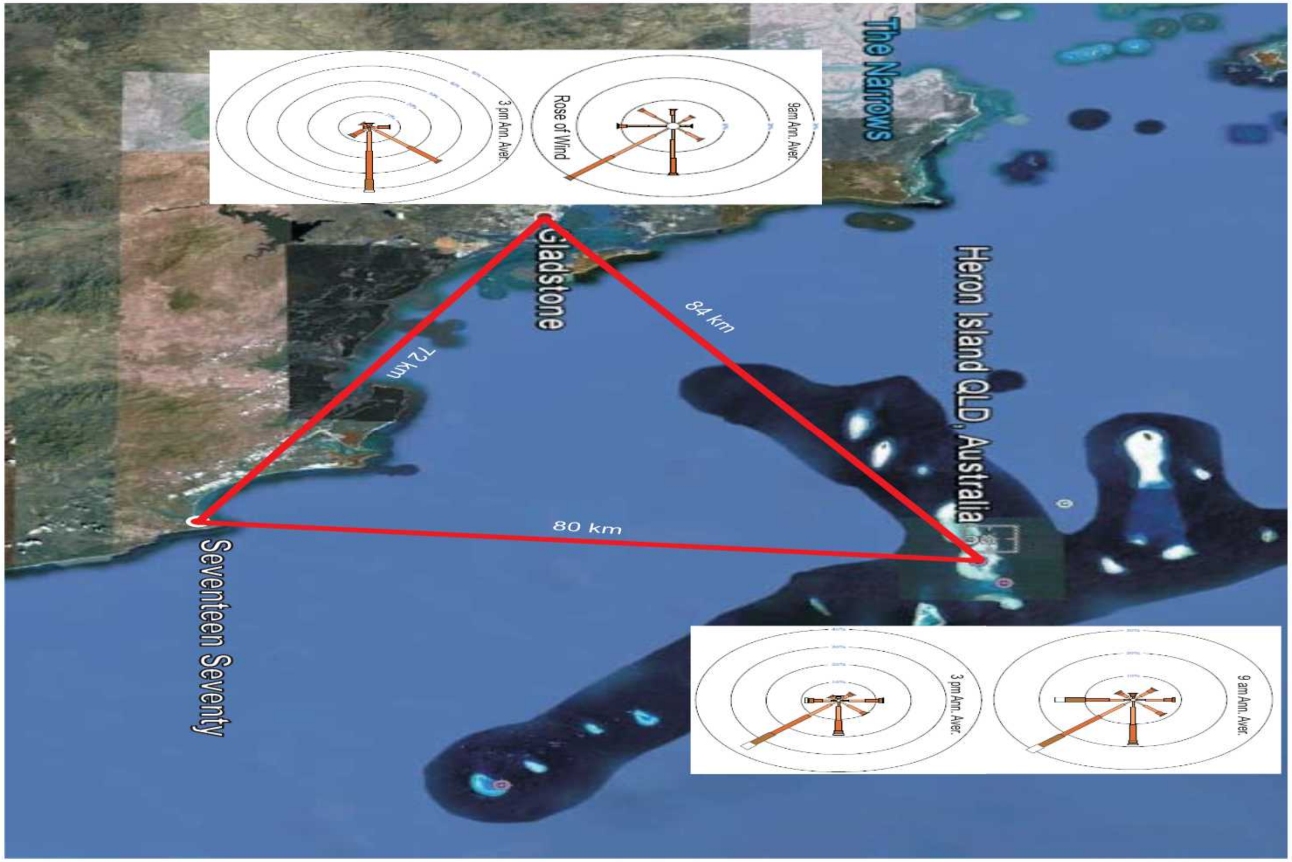

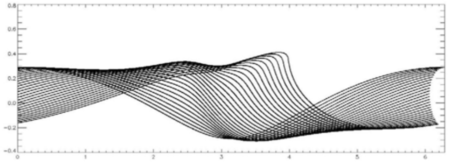

Wave asymmetry at extreme wind forcing

- Leikin et al., 1995, *Nonlinear Proc. Geophys*., laboratory experiment with wind-forced waves
- Strong correlation of asymmetry A_s with wind forcing, no correlation for skewness and steepness
- Broad range of u_* which converts into U_{10}=8-48m/s
- Asymmetry saturates at u_*/c_p~1.2, i.e. at

  U_{10}~34m/s
- This indicates change of the wave breaking mechanism to, perhaps, breaking due to direct wind forcing

Air-Sea Gas Exchanges in Extreme Conditions

- McNeil & D' Asaro, 2007, *J. Mar. Scie.*
- cross-interface gas fluxes measured during Hurricane Frances in 2004
- U_{10} up to 55m/s
- fluxes still grow, but at a slow rate if

$$U_{10} > 35\text{m/s}$$

- additional mechanism of air injection due to bubbles of 1mm diameter transported down to 20m below the surface and dissolved due to the hydrostatic compression

Yasi – inner grid

- DOUBLE HOLLAND parametric winds (left) and WRF winds (right) for 2 Feb 2011 10:00UTC

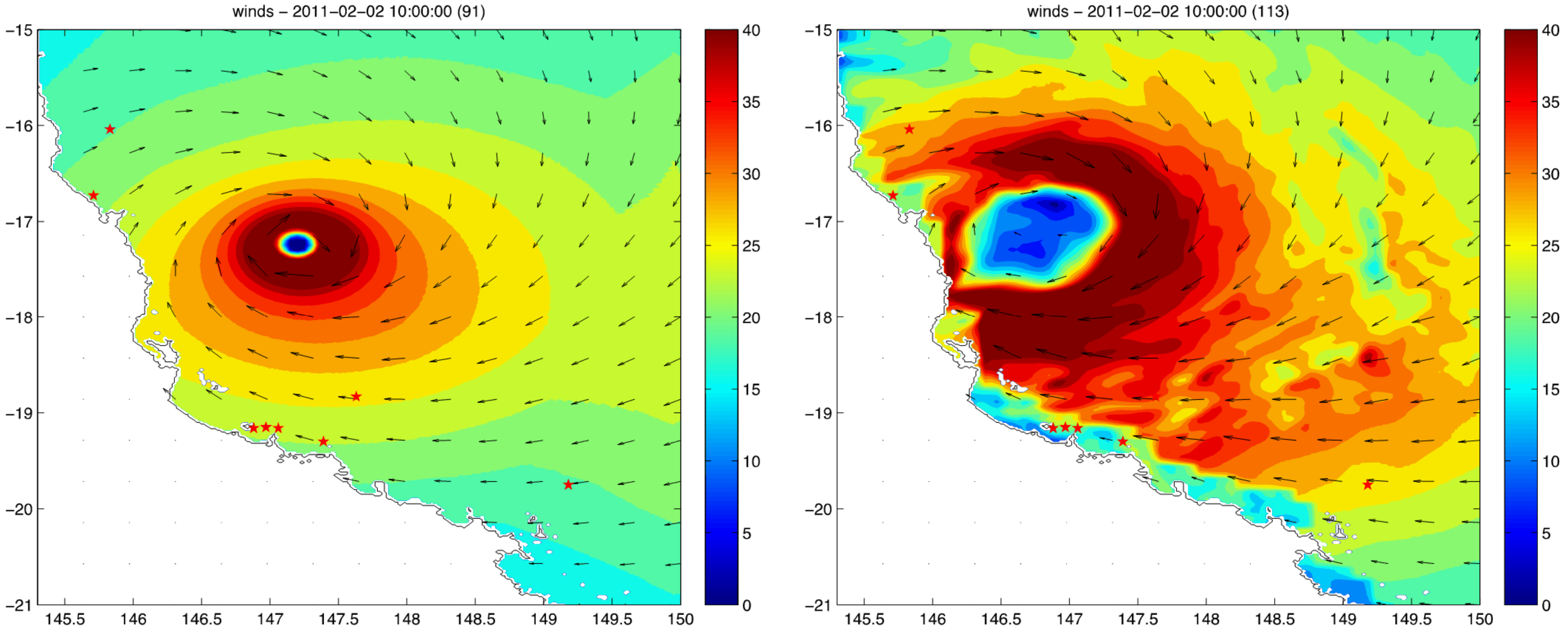

Yasi – inner grid

- wave height from DOUBLE HOLLAND parametric winds (left) and WRF winds (right) for 2 Feb 2011 10:00UTC

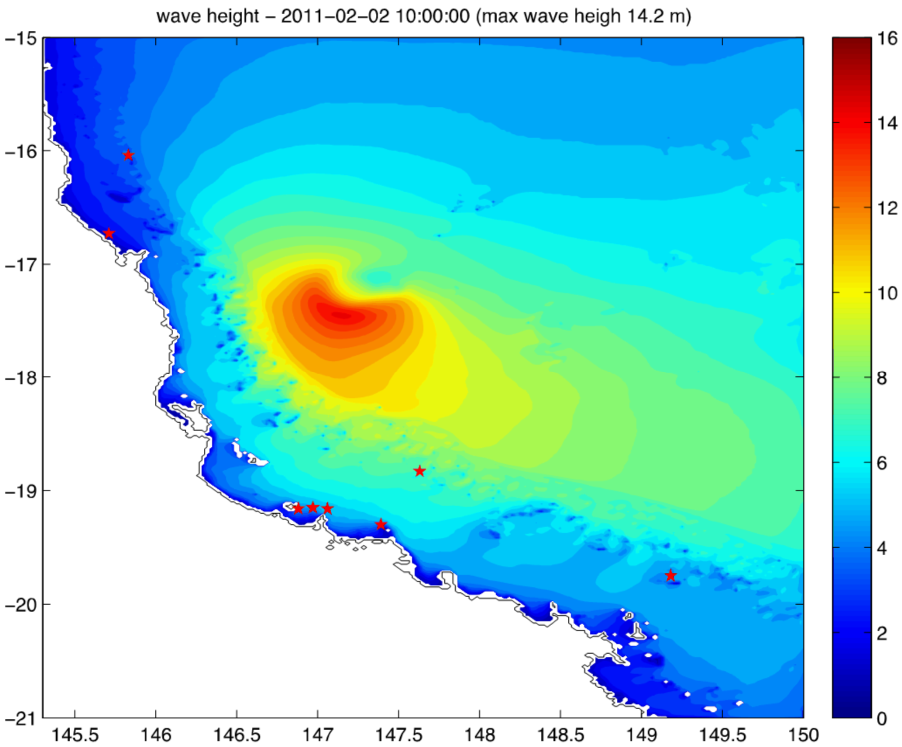

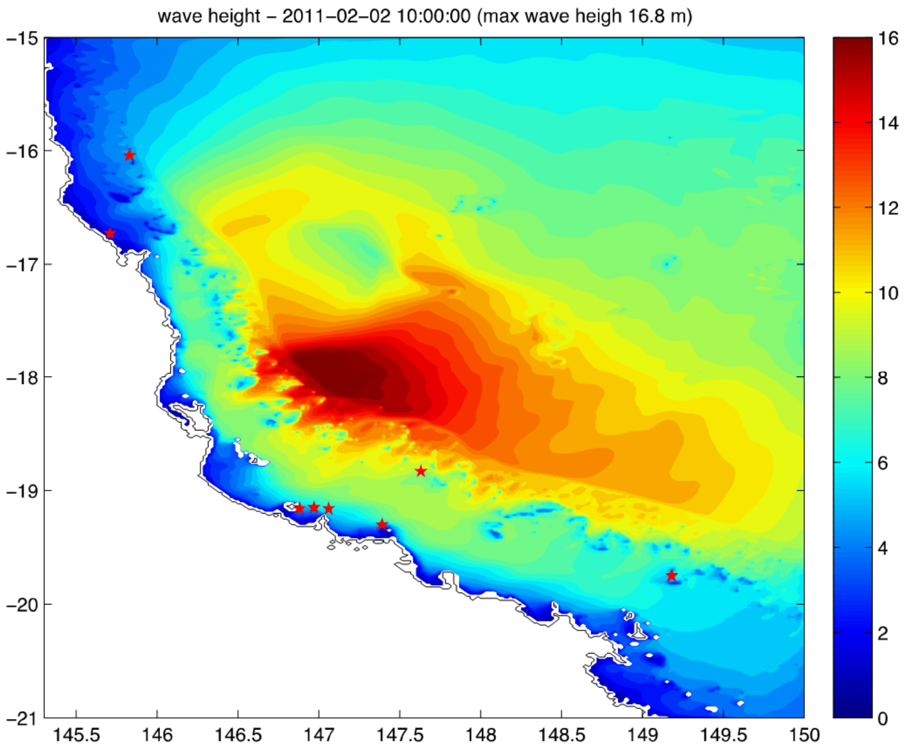

Hypothesis of the Wave Reynolds Number

Babanin, GRL, 2006

$\eta(x,t) = a_0\cos(\omega t+kx)$

$a(z) = a_0\exp(-kz)$

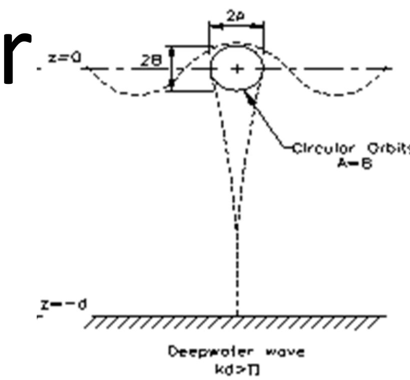

It is the hypothesis that the a-based Reynolds number

$$\mathrm{Re} = \frac{aV}{\nu} = \frac{a^2\omega}{\nu}$$

where $V=\omega a$ is orbital velocity, and ν is kinematic viscosity of the ocean water, indicates transition from laminar orbital motion to turbulent

Critical Reynolds Number for the Wave-Induced Motion, and Depth of the Mixed Layer

$$\mathrm{Re}(z) = \frac{\omega}{\nu} a_0^2 \exp(-2kz) = \frac{\omega}{\nu} a_0^2 \exp(-2\frac{\omega^2}{g} z)$$

$$z_{cr} = -\frac{1}{2k}\ln(\frac{\mathrm{Re}_{cr}\,\nu}{a_0^2\omega}) = \frac{g}{2\omega^2}\ln(\frac{a_0^2\omega}{\mathrm{Re}_{cr}\,\nu})$$

Re_{cr}=3000

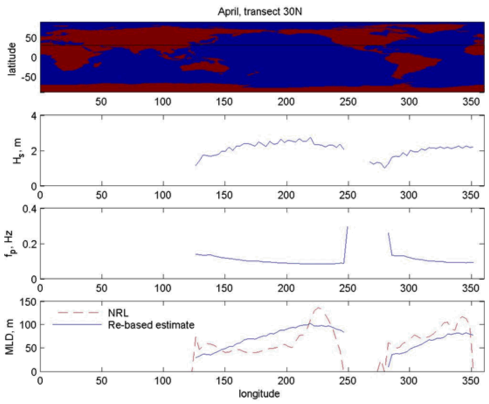

Potential role of the wave-induced mixing

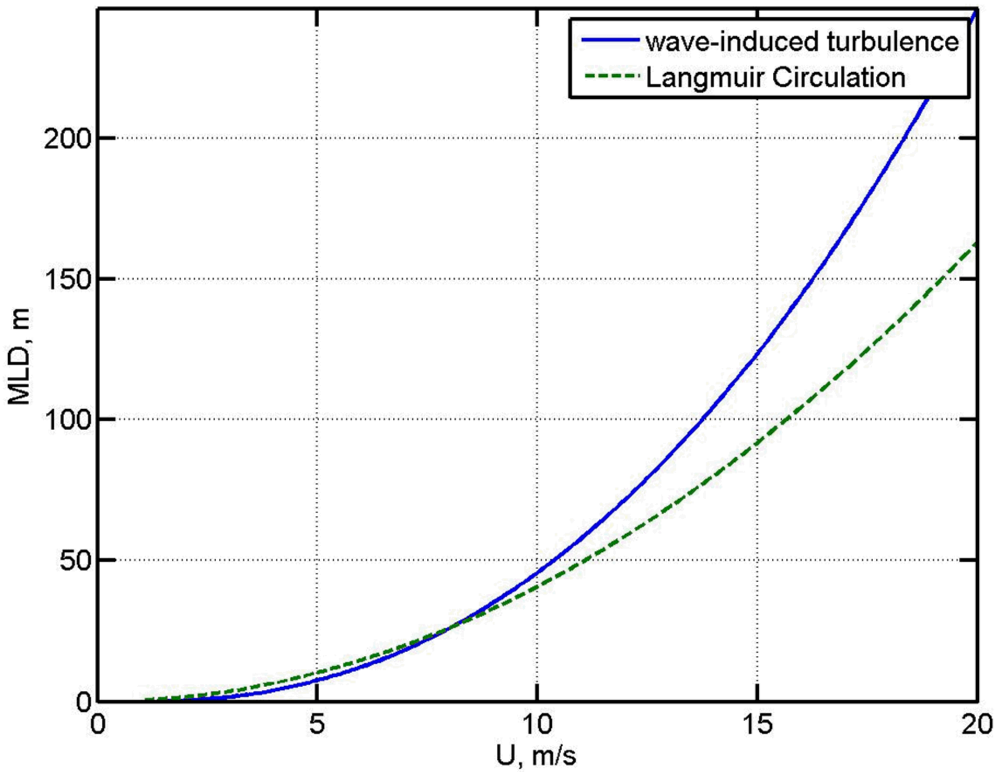

Wave turbulence

$$z_{cr} = \frac{g}{2\omega^2} \ln\left(\frac{a_0^2 \omega}{\mathrm{Re}_{cr}\, \nu}\right)$$

$$\omega = 0.819 \frac{g}{U_{10}},$$

$$a_0 = 0.121 \frac{U_{10}^2}{g},$$

Langmuir circulation

$H_L = 4U^2{}_{10}/g$

Babanin et al., 2009, Ocean Modelling

Dai et al., JPO, 2010

Laboratory Experiment in the First Inst. of Oceanography, China

Mixing the stratified fluid
experiment (left), model (right)

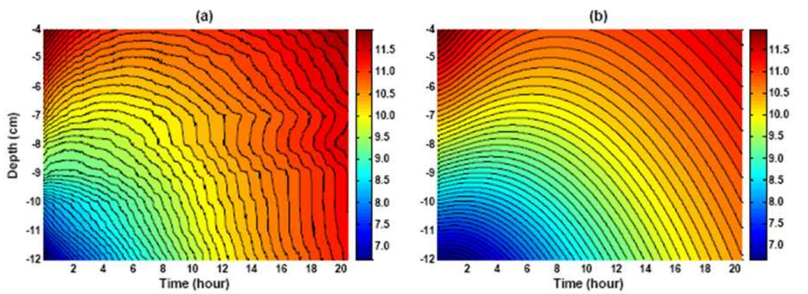

Figure 2. Evolution of the water-temperature profile without waves. (a) observations; (b) numerical simulation with the one-dimensional model. The time is in hours.

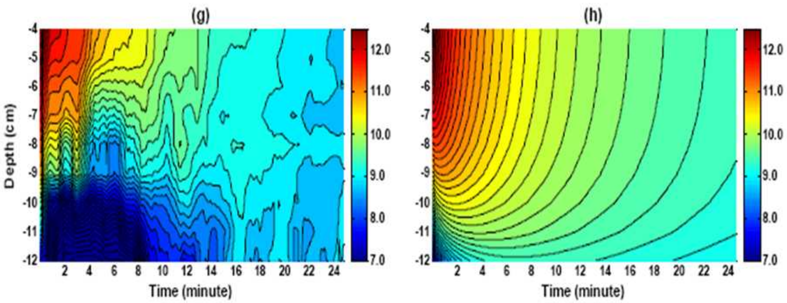

no waves
time scale: hours

non-breaking waves
time scale: minutes

Laboratory Experiment at ASIST, RSMAS, University of Miami

turbulence is highly intermittent, most frequent at rear wave face

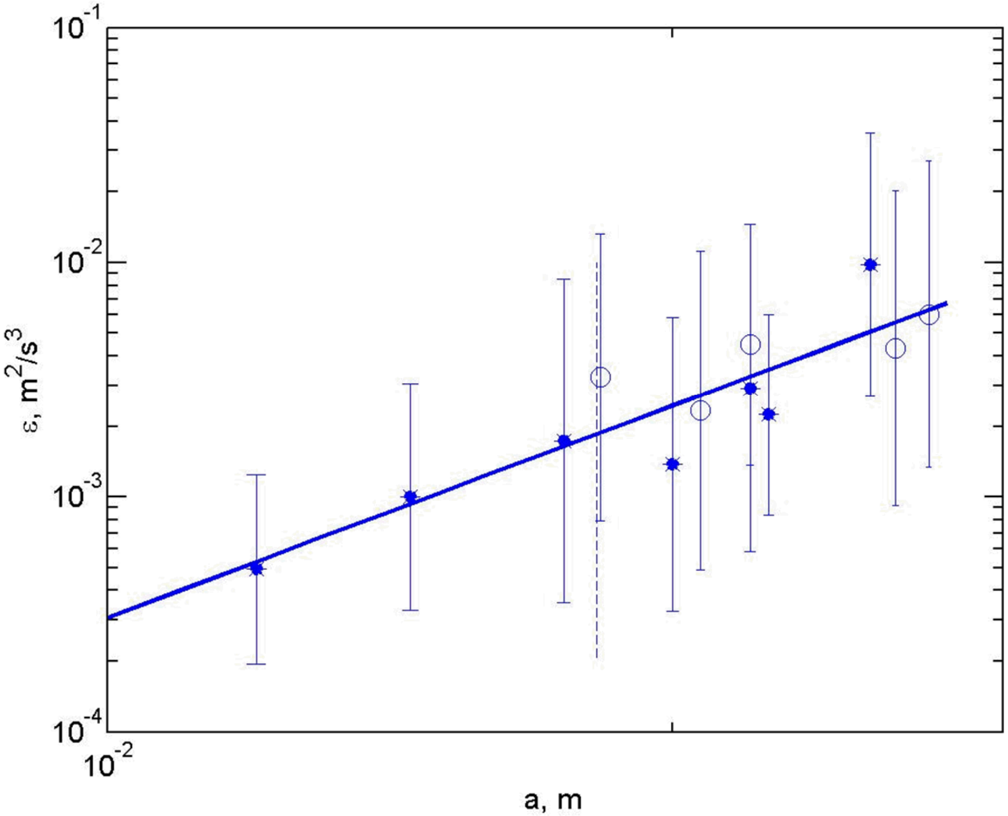

$$\varepsilon = 300 \cdot a^{3.0 \pm 1.0}$$

This is close to the expectation: since the force due to the turbulent stresses is proportional to a^2, the energy dissipation rate should be ~a^3.

Babanin and Haus, 2009

Babanin & Chalikov, JGR, submitted

Model of generation of turbulence by nonlinear waves

Model is based on exact 2-D (x-z) model of surface waves coupled with 3-D LES (x-y-z) model of vortical motion based on Reynolds equation with parameterised subgrid turbulence.

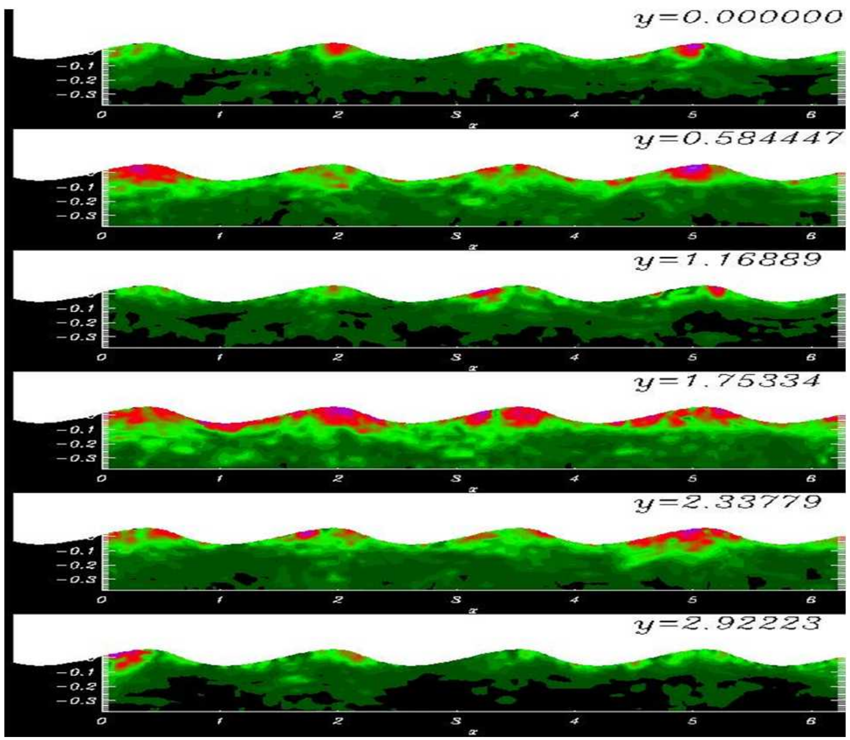

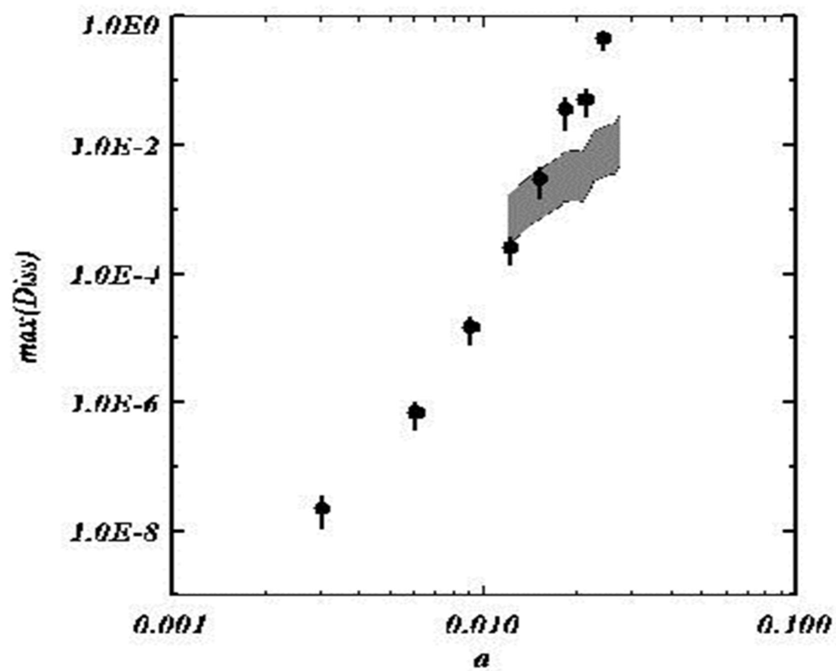

Pleskachevski et al., JPO, 2010

Field observations, North Sea, sediment suspension

$$\frac{\partial K}{\partial T_{mean}} + U_i \frac{\partial K}{\partial X_i} = D_K + P_S + G - E_K$$

TKE evolution equation

$$P_s = P_{CURR} = \upsilon_t M^2_{CURR}$$

TKE production

$$M = \partial \bar{u}_i / \partial x_j$$

shear frequency

$$P_s = (\upsilon_{CURR} + \upsilon_{wave})(M^2_{CURR} + M^{AM\ 2}_{wave})$$

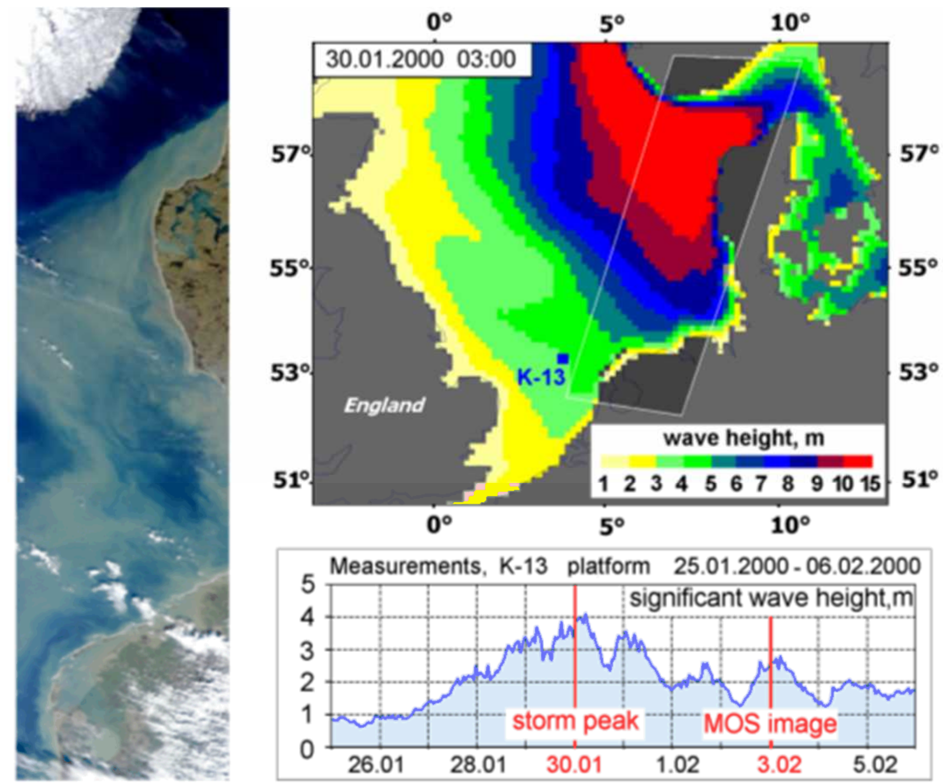

FIG. 1. Storm events in the North Sea at 29.01-04.02.2000 (the storm peak on 30.01.2000, at about 03:00 UTC). Optical MOS image of German Bight on 03.02.2000 (left) and significant wave height in the North Sea at the storm peak (right).

Toffoli et al., JGR, submitted

Field observations, North Rankin mixed layer deepening

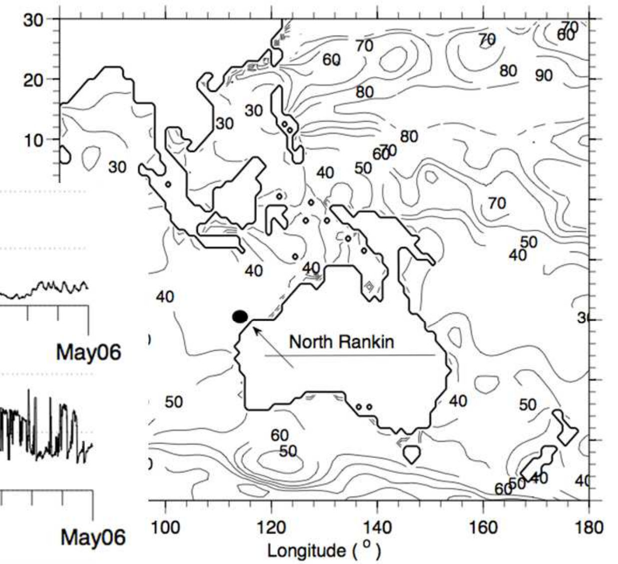

Wave height

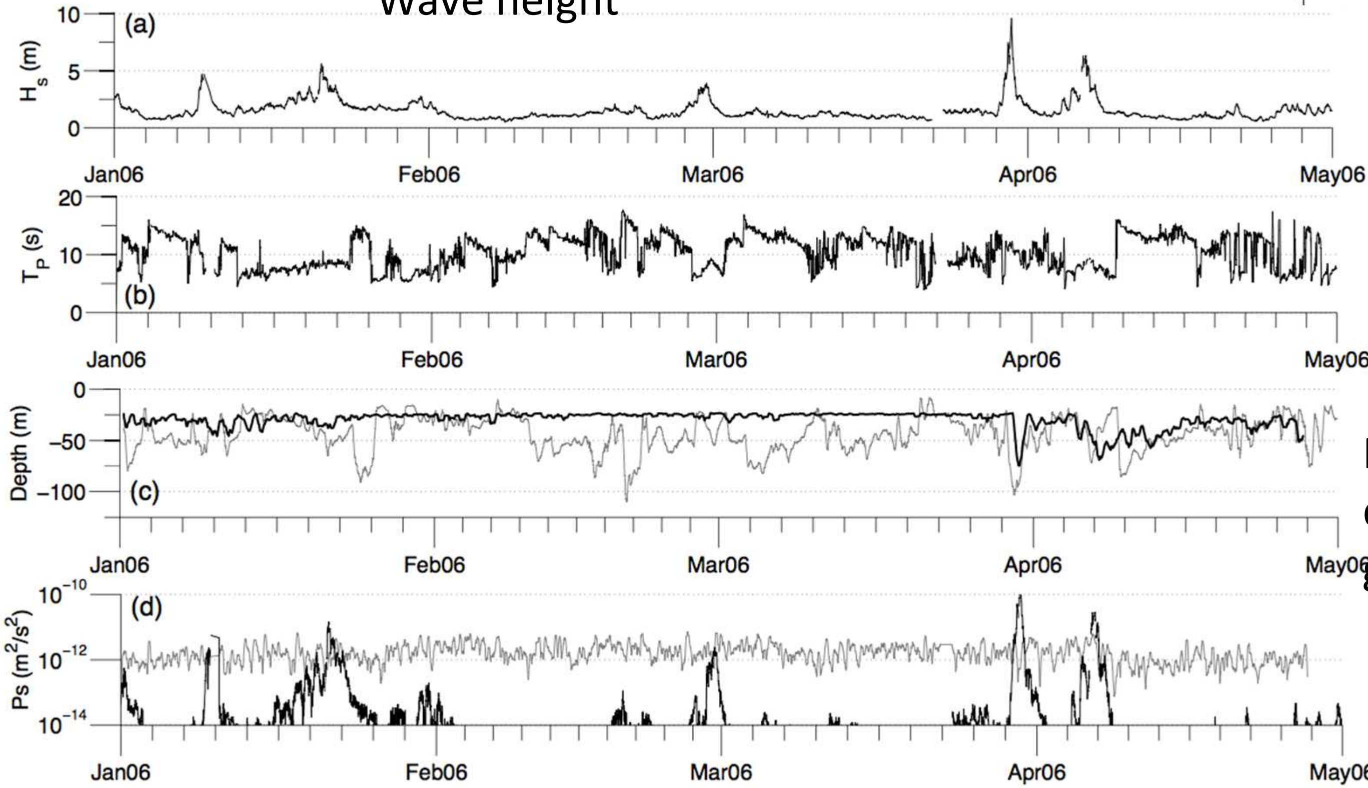

MLD:
dark – wave induced
grey - measured

Ghantous et al., Ocean Modelling, submitted

Modelling SST and MLD at the scale of tropical cyclone

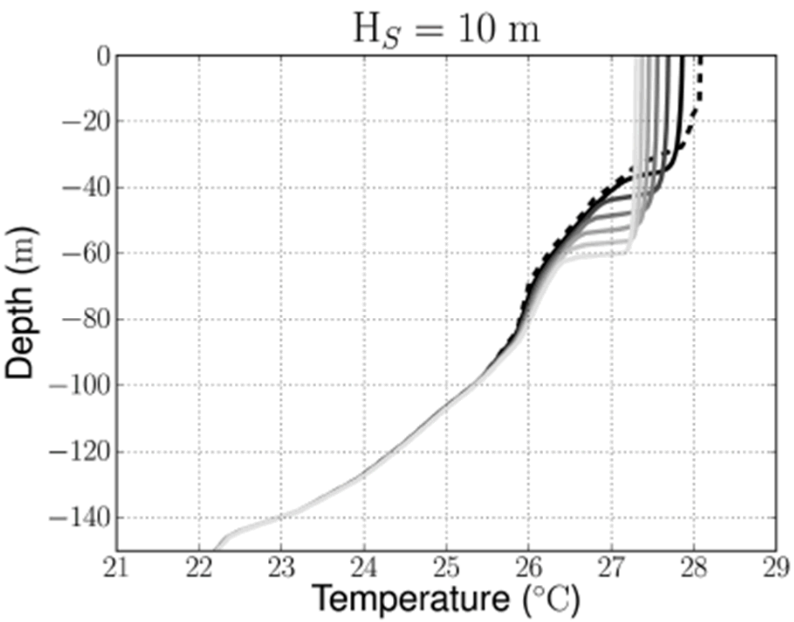

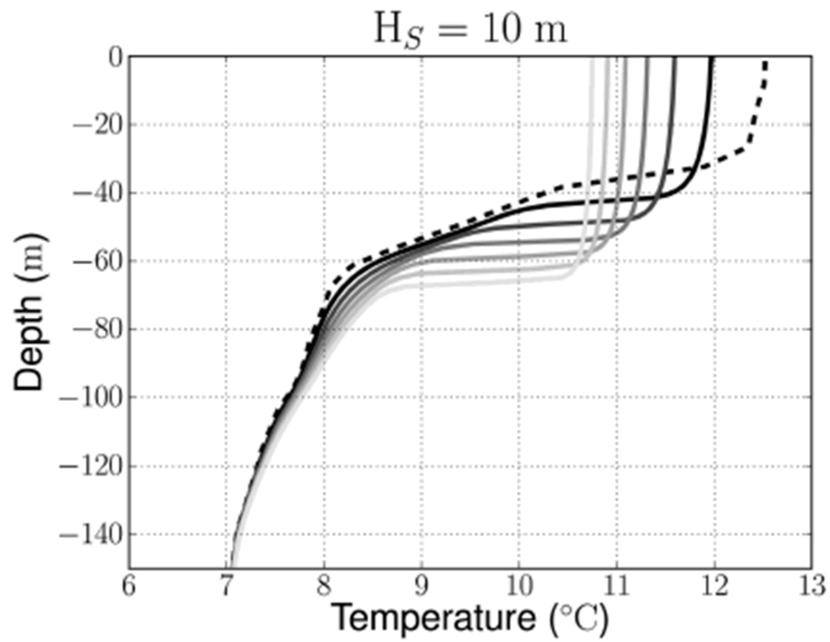

Implementing wave-induced mixing in CLIMBER

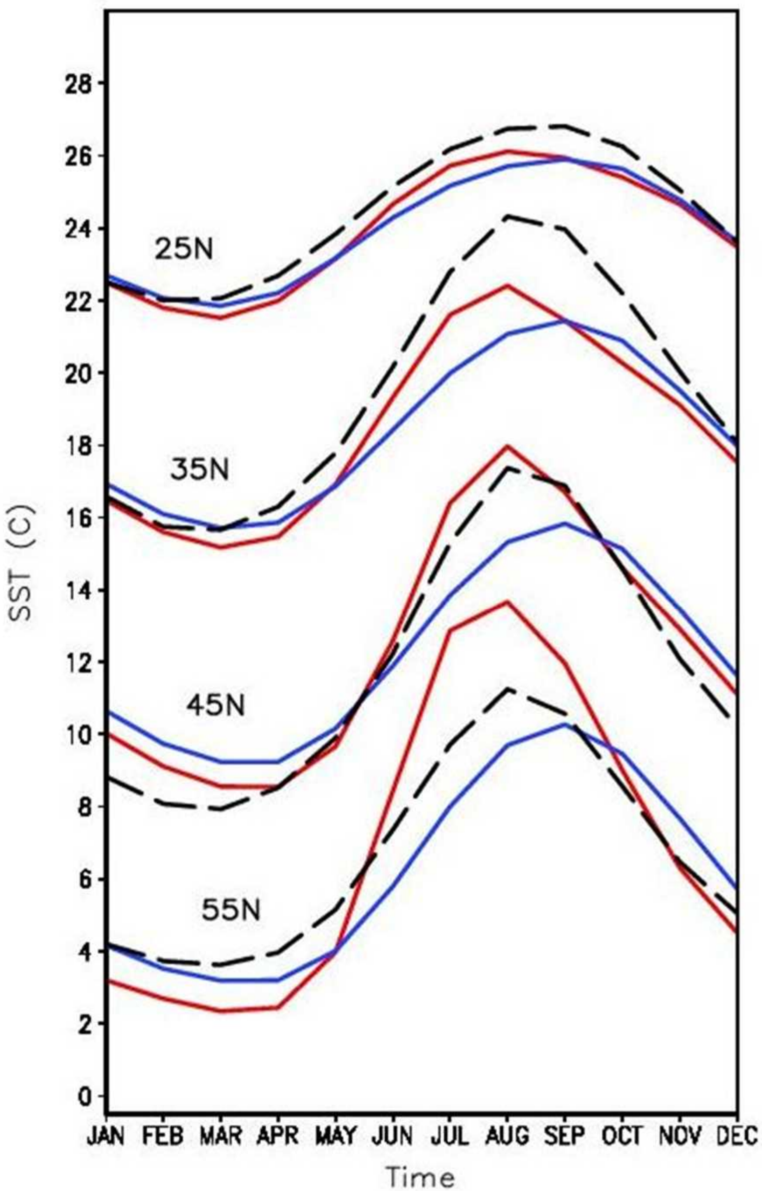

- Seasonal trend of the global zonally averaged SST. Panels shown: 25, 35, 45 and 55 degrees North (from top to bottom). Lines shown: default version of CLIMBER (blue), variable MLD (red) and observations based on Levitus data (black).
- effect is essential outside the tropical areas
- both magnitudes and phases of SST are imporved

Implementing wave-induced mixing in CLIMBER

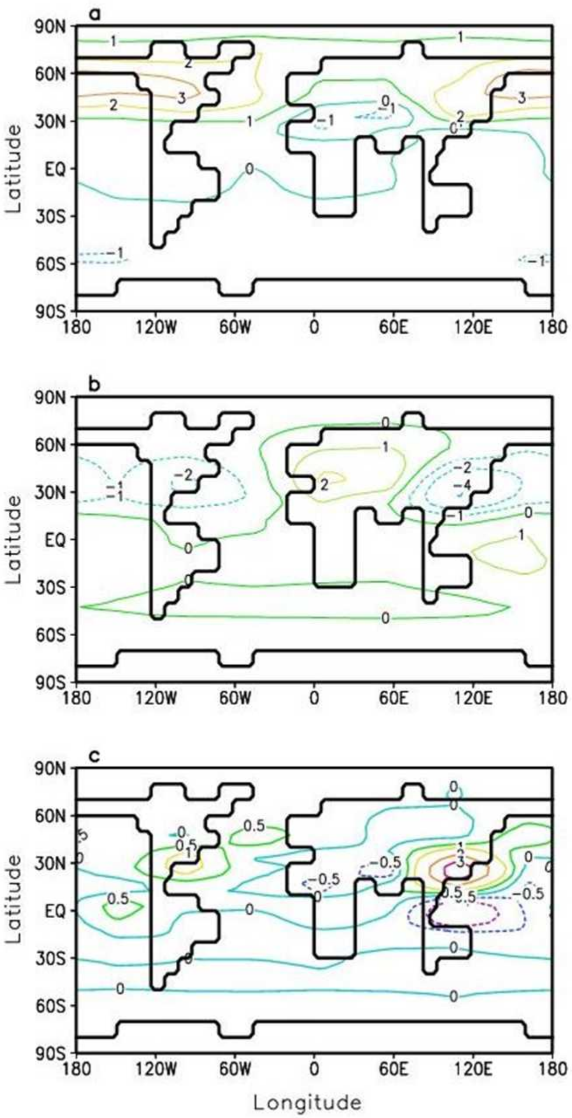

Global distribution (Northern summer)

- temperature (*degrees*)
- pressure (*mbar*)
- precipitation (*mm* per day)

Wave-Induced Turbulence in ocean models

Qiao et al., 2010, Ocean Dynamics

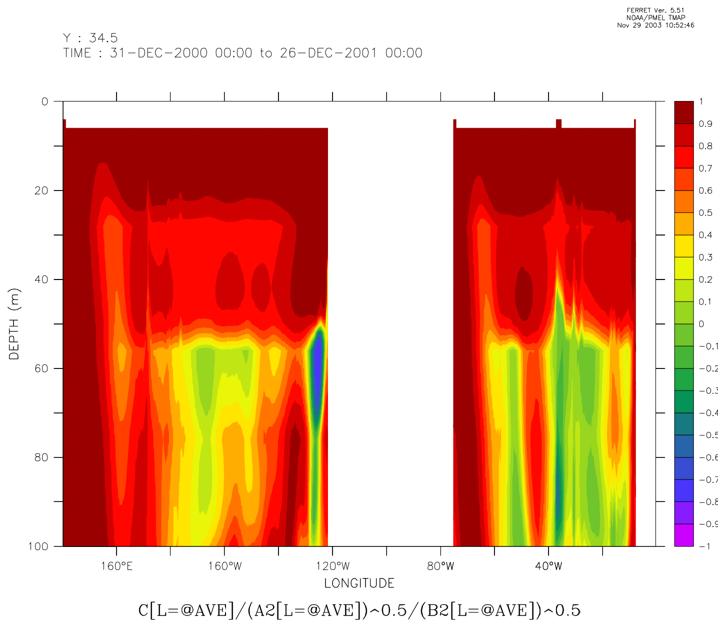

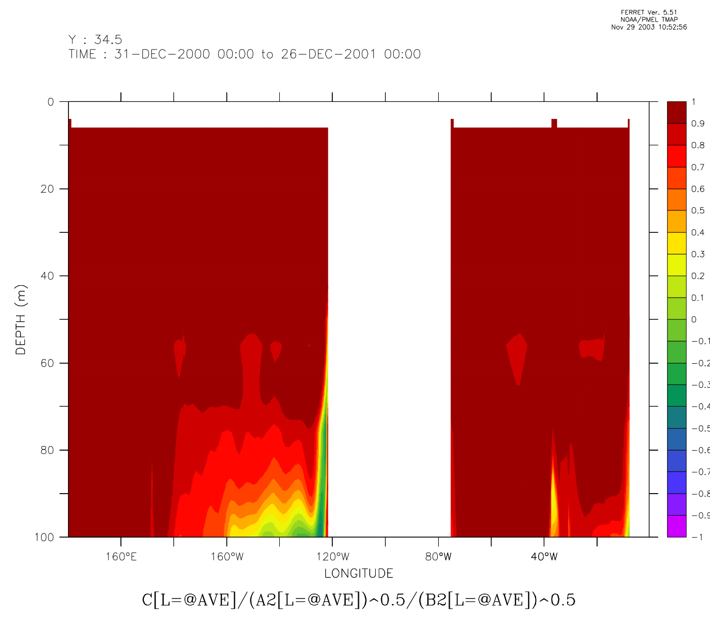

Correlation coefficients between the model outcomes and the World Ocean Atlas for vertical temperature distributions at 35N latitude (darker areas correspond to higher correlation. The left panel demonstrates the transect across the Pacific (left) and Atlantic (right) oceans without wave-induced turbulent stresses accounted for, and the right panel – with the respective Reynolds stresses added.

Qiao at al., 2010 Globally averaged SST

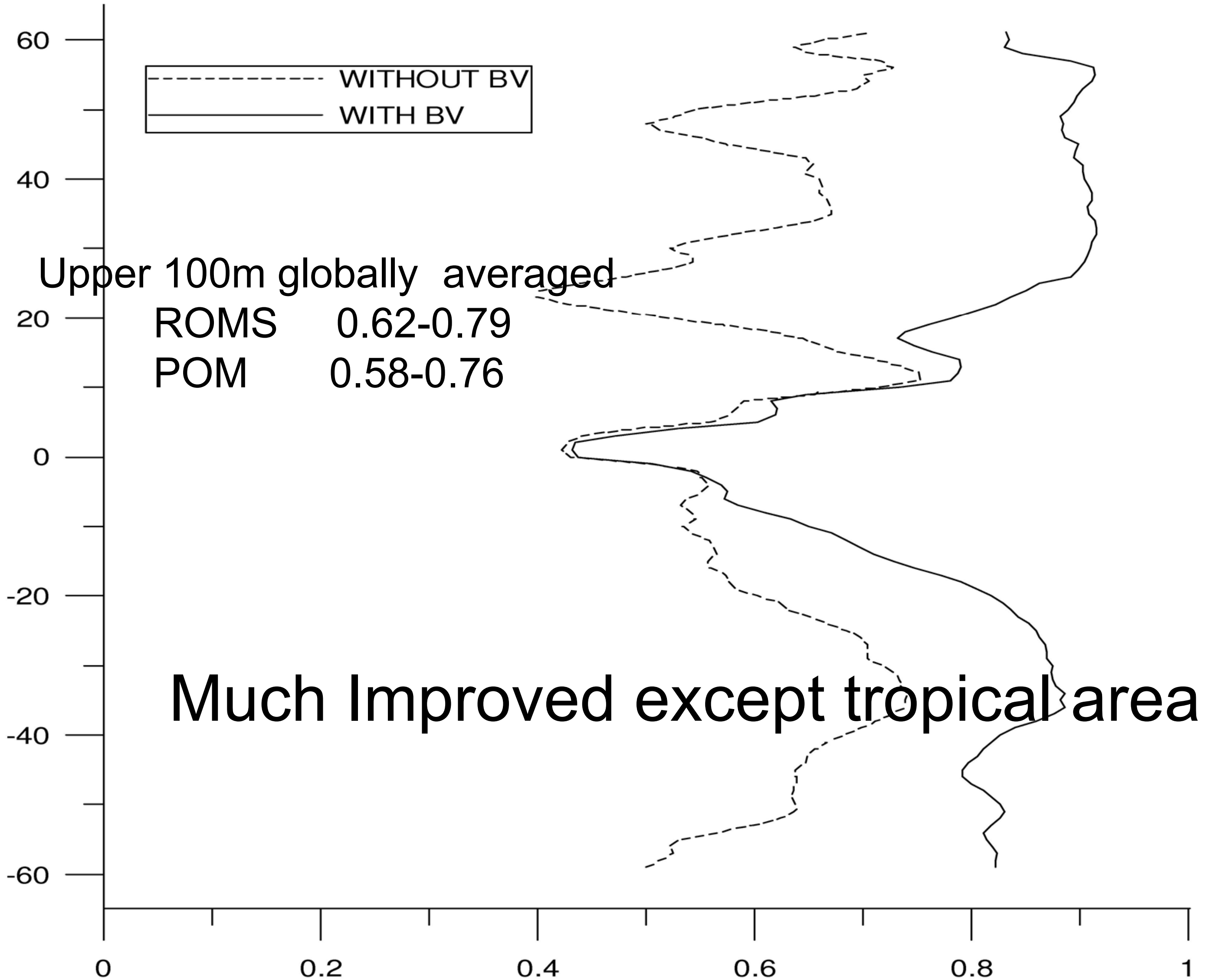

Motivation

Waves influences the climate, climate affects the waves

Winds and waves change

Observations

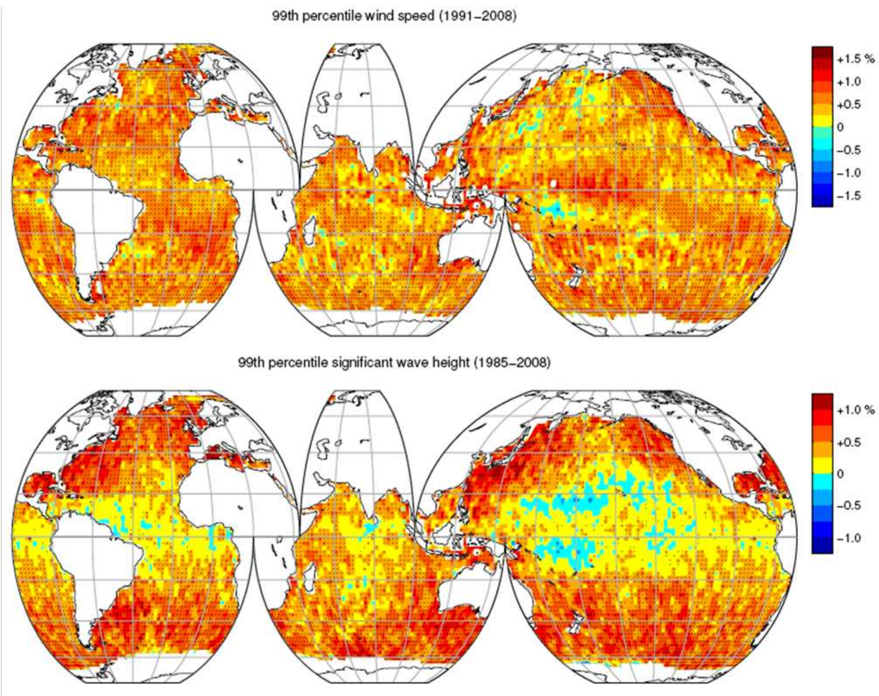

Young et al., Science, 2011

Sea surface temperature changes due to waves

Model

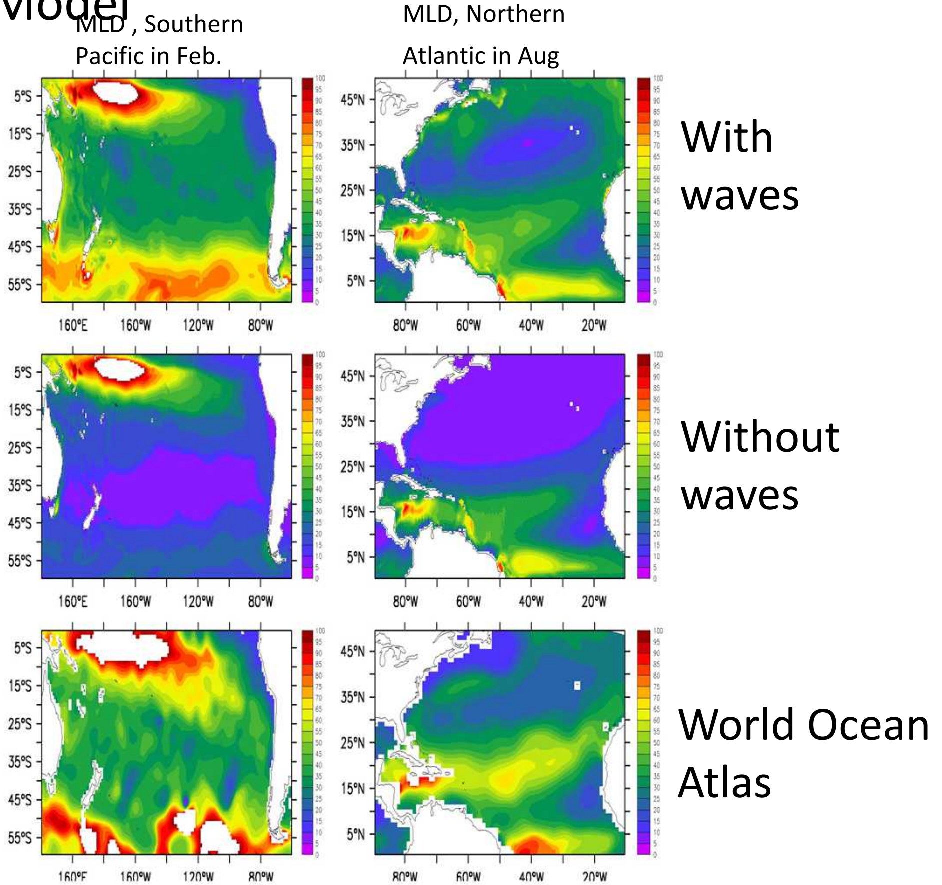

Qiao et al., Ocean Dynamics, 2010